

# Mountaineering Strategy to Excited States: Highly Accurate Oscillator Strengths and Dipole Moments of Small Molecules

Amara Chrayteh, Aymeric Blondel, Pierre-François Loos, and Denis Jacquemin\*

Cite This: *J. Chem. Theory Comput.* 2021, 17, 416–438

Read Online

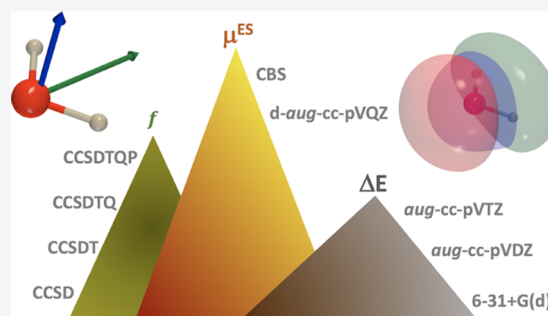
ACCESS |

Metrics & More

Article Recommendations

Supporting Information

**ABSTRACT:** This work presents a series of highly accurate excited-state properties obtained using high-order coupled-cluster (CC) calculations performed with a series of diffuse containing basis sets, and extensive comparisons with experimental values. Indeed, we have computed the main ground-to-excited transition property, the oscillator strength, and the ground- and excited-state dipole moments, considering 13 small molecules (hydridoboron, hydrogen chloride, water, hydrogen sulfide, boron fluoride, carbon monoxide, dinitrogen, ethylene, formaldehyde, thioformaldehyde, nitroxyl, fluorocarbene, and silylidene). We systematically include corrections up to the quintuple (CCSDTQP) in the CC expansion and extrapolate to the complete basis set limit. When comparisons with experimental measurements are possible, that is, when a number of consistent experimental data can be found, theory typically provides values falling within the experimental error bar for the excited-state properties. Besides completing our previous studies focused on transition energies [*J. Chem. Theory Comput.* 14 (2018) 4360–4379, *ibid.* 15 (2019) 1939–1956, *ibid.* 16 (2020) 1711–1741, and *ibid.* 16 (2020) 3720–3736], this work also provides ultra-accurate dipoles and oscillator strengths that could be employed for future theoretical benchmarks.



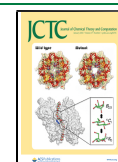
## 1. INTRODUCTION

In the formidable quest aiming at reaching high accuracy in the modeling of electronically excited states (ESs), the primary focus has been set on vertical excitation energies,<sup>1</sup> defined as the difference in total energies between a given ES and its corresponding ground state (GS) at fixed geometry (typically the GS equilibrium geometry). The main reasons for this choice are, on the one hand, the availability of many theoretical models for computing total ES energies and, on the other hand, the fact that obtaining accurate transition energies is generally viewed as a prerequisite for further ES investigations. Along the years, more and more accurate vertical transition energies have become available. Probably the most illustrative examples are provided by the well-known Thiel set,<sup>2–4</sup> encompassing 223 values obtained at the CC3 and CASPT2 levels and our recent efforts to obtain chemically accurate vertical energies within  $\pm 0.03$  eV of the full configuration interaction (FCI) limit for more than 400 ES.<sup>5–8</sup> Although such sets are obviously useful to benchmark lower-order methods, they remain, nevertheless, intrinsically limited by two factors. First, vertical transition energies remain inaccessible experimentally (in the vast majority of the cases), preventing direct comparisons with measurements. To circumvent this issue, several groups have turned their attention to 0–0 energies,<sup>9–23</sup> defined as the differences between the ES and GS energies determined at their respective minimum and corrected for zero-point vibrational effects, because 0–0 energies allow straightforward theory–experiment compar-

isons. To compute 0–0 energies, one must, however, determine ES geometries and vibrations, which limits the number of methods that can be applied. This explains why compromise “hybrid” protocols employing different levels of theory for the structural and energetic parameters are popular in this particular field.<sup>12,18,19,21</sup> Interestingly, the accuracy of the underlying geometries has been shown to be rather irrelevant,<sup>14,22</sup> indicating that benchmarks of 0–0 energies still mainly assess the quality of the (adiabatic) transition energies. Second, vertical transition energies provide only a very partial characterization of the ES as one typically needs to determine transition probabilities (oscillator strengths,  $f$ ) and ES properties (such as structures and dipole moments,  $\mu$ ) to attain a better grasp of the photophysics. On a more theoretical viewpoint, it is also known that a method can provide accurate transition energies while failing to deliver accurate ES properties,<sup>24–26</sup> indicating that benchmarks relying on transition energies as unique gauge can lead to incomplete and/or erroneous conclusions regarding the strengths and weaknesses of a given theoretical model.

Received: October 22, 2020

Published: December 1, 2020



In the above-defined framework, let us now summarize the efforts that have been made to define accurate reference ES properties for significant sets of compounds.

First, for ES geometries, which are not our focus here, several ensembles of structures have been reported at CASPT2,<sup>27</sup> SAC-CI,<sup>28,29</sup> Mk-MRCCSD,<sup>30</sup> QMC,<sup>31</sup> and CC2<sup>32</sup> levels. To the best of our knowledge, the most extensive dataset of accurate ES structural parameters remains the one defined by some of us during the last few years: it contains bond lengths, valence angles, and torsion angles determined at the CC3 and CASPT2 levels with aug-cc-pVTZ for several dozens of small organic compounds.<sup>22,24,33–35</sup> In this framework, it is also worth mentioning the studies of Szalay's group on the shape of potential energy surfaces, in which CCSDT references are defined,<sup>25,26,36</sup> and the publications of Olivucci's group focusing on the topology of conical intersections, in which the results of high-level multireference calculations are provided.<sup>37,38</sup>

Second, for transition properties, the most accurate reference values we are aware of (for a significant set of transitions) are (i) the CC3/TZVP oscillator strengths obtained by Kánnár and Szalay<sup>39</sup> for the Thiel set (this work also includes 15 CCSDT/TZVP oscillator strengths) that can be compared to CASPT2/TZVP values obtained earlier for the same set;<sup>2</sup> (ii) the numerous CC3/aug-cc-pVTZ oscillator strengths determined to complete our FCI energy calculations;<sup>5,7,8</sup> and (iii) the transition dipole moments computed at the CC3 or ADC(3) levels for 15 molecules by Robinson.<sup>40</sup> There are also earlier sets of oscillator strengths computed at lower levels of theory, for example, CCSD,<sup>41</sup> SAC-CI,<sup>42</sup> and CC2.<sup>43,44</sup> The typical error associated with these approaches (with respect to FCI) remains unknown at this stage. To the best of our knowledge, a significant set of FCI-quality oscillator strengths is yet to be published.

Third, theoretical datasets for accurate ES dipoles are apparently even scarcer. The most advanced sets we are aware of contain (i) CASPT2/TZVP<sup>2</sup> and CC2/aug-cc-pVTZ reference values<sup>43</sup> determined for the Thiel set; (ii) CC2/aug-cc-pVQZ results for small- and medium-sized molecules;<sup>45</sup> and (iii) CC2/aug-cc-pVTZ data for “real-life” organic dyes.<sup>46</sup> Comparisons with experimental ES dipoles performed in ref 45 yield an error of *ca.* 0.2 D for both ADC(2) and CC2, a value that can be viewed as acceptable, but is nevertheless far from chemical accuracy and not on par with the precision provided by state-of-the-art approaches for GS dipole moments.<sup>47</sup> Of course, one can find specific studies focusing on a small number of ES dipoles and using a high level(s) of theory (see our Results and Discussion section for references). However, such specific studies preclude valuable statistical conclusions.

Globally, these previous studies have demonstrated that both  $f$  and  $\mu^{\text{ES}}$  are much more basis set-sensitive than transition energies and geometries. Indeed, a specific challenge comes from intensity-borrowing effects that can vastly change the properties of two close-lying ESs of the same symmetry while their energies remain almost unaffected. When a change in basis set slightly tunes the energy gap between two ESs, it might simultaneously drastically affect the properties. This highlights that properties are much harder to accurately estimate than energies, not only for implementation or computational reasons but also due to more fundamental aspects.

Another important fact is that in contrast to vertical transition energies, both oscillator strengths and ES dipole

moments are accessible experimentally, so comparisons between theoretical and experimental measurements are, in principle, possible. However, as we pointed out previously for geometries,<sup>33</sup> such comparisons are generally far from straightforward. For the oscillator strengths, the two main measurement techniques are electron impact and optical spectroscopies. As nicely summarized elsewhere,<sup>48</sup> the former typically requires extrapolations of the cross-sections measured at various momenta/angles (such extrapolations are not error-free), whereas the latter can be plagued by saturation and interaction effects (yielding to underestimation of the actual  $f$  value). In any case, the so-called “electronic” or “optical”  $f$ , which is of interest here, is not directly measurable, and postprocessing of the experimental raw data (lifetimes or cross sections) is needed to access its “experimental” value.<sup>48,49</sup> The measurements of ES dipoles are also cumbersome.<sup>50</sup> The typical strategy is to investigate solvatochromism, that is, to measure the shift of the emission wavelength in a series of solvents of various polarities, and to fit the results with the Lippert–Mataga equation within an Onsager-like interaction model. Such an approach is obviously not a direct gas-phase measurement and comes with significant assumptions, making the final error often too large to allow benchmarking.<sup>51</sup> Alternatively, one can also measure  $\mu^{\text{ES}}$  directly in gas phase by studying how external electric fields tune the position and shape of the vibronic peaks (the so-called Stark effect).<sup>50,51</sup> Only the latter approach can be considered as sufficiently robust for reference purposes. Still, such Stark effect measurements do typically provide an “adiabatic” version of  $\mu^{\text{ES}}$ , that is, the ES dipole measured at the ES equilibrium geometry. If a nontrivial structural reorganization takes place after absorption, such as in formaldehyde, this means that the value of  $\mu^{\text{ES}}$  computed at the GS equilibrium structure has again no experimental counterpart. In addition, the direction of the ES dipole moment cannot be determined directly from the measurements of the Stark effect.

For all these reasons, it is of interest to define a set of coherent near-FCI oscillator strengths and ES dipole moments. Indeed, the oscillator strengths are directly related to the transition dipole moments, whereas the dipole moments can be seen as a measure of the quality of the total (GS and ES) densities, so that these data go beyond the “simple” characterization of vertical transition energies. This contribution therefore aims at tackling this ambitious objective for a set of small molecules similar to the one treated in our original mountaineering paper.<sup>5</sup> To this end, we take advantage of the CC hierarchy, going from CCSD to CCSDTQP for both properties, in combination with increasingly large atomic basis sets including one or two sets of diffuse basis functions. Although such calculations provide “definite answers”, they remain at the limit of today's computational capabilities and are achievable for compact molecules only, which stands as a clear limit of the present contribution. Nevertheless, providing highly accurate numbers for properties directly related to the quality of the transition and the ES densities is, we believe, useful. Very recently, Hait and Head-Gordon have used, in a density-functional theory (DFT) context, the GS dipole moment as a metric to estimate the quality of the GS density given by many exchange–correlation functionals.<sup>47</sup> As these authors nicely stated, the dipole “*is perhaps the simplest observable that captures errors in the underlying density, (...and is) a relevant density derived quantity to examine for DFA testing and development*”. The extension to ESs (and time-dependent

Table 1. GS Dipole Moment  $\mu^{\text{GS}}$ , Vertical Transition Energies  $\Delta E_{\text{vert}}^{\text{ES}}$ , Vertical Oscillator Strengths  $f$ , and ES Dipole Moments,  $\mu_{\text{vert}}^{\text{ES}}$  and  $\mu_{\text{adia}}^{\text{ES}}$ , Determined for BH (GS and ES Geometries) and HCI (GS Geometry)<sup>a</sup>

| basis         | method           | BH                       |                                      |                    | HCI                |                                      |                            |
|---------------|------------------|--------------------------|--------------------------------------|--------------------|--------------------|--------------------------------------|----------------------------|
|               |                  | $\mu^{\text{GS}}$        | $\Delta E_{\text{vert}}^{\text{ES}}$ | $f$                | $\mu^{\text{GS}}$  | $\Delta E_{\text{vert}}^{\text{ES}}$ | $f$                        |
| aug-cc-pVDZ   | CCSD             | 1.389                    | 2.970                                | 0.051              | 1.147              | 7.862                                | 0.066                      |
|               | CCSDT            | 1.371                    | 2.946                                | 0.049              | 1.131              | 7.815                                | 0.065                      |
|               | CCSDTQ           | 1.370                    | 2.947                                | 0.049              | 1.130              | 7.822                                | 0.065                      |
|               | CCSDTQP          | 1.370                    | 2.947                                | 0.049              | 1.130              | 7.823                                | 0.065                      |
| aug-cc-pVTZ   | CCSD             | 1.433                    | 2.928                                | 0.050              | 1.097              | 7.906                                | 0.056                      |
|               | CCSDT            | 1.410                    | 2.900                                | 0.048              | 1.085              | 7.834                                | 0.055                      |
|               | CCSDTQ           | 1.409                    | 2.901                                | 0.048              | 1.084              | 7.837                                | 0.055                      |
| aug-cc-pVQZ   | CCSD             | 1.440                    | 2.918                                | 0.050              | 1.111              | 7.954                                | 0.051                      |
|               | CCSDT            | 1.416                    | 2.890                                | 0.048              | 1.098              | 7.880                                | 0.050                      |
| aug-cc-pVSZ   | CCSD             | 1.443                    | 2.915                                | 0.050              | 1.109              | 7.961                                | 0.048                      |
|               | CCSDT            | 1.388                    | 2.969                                | 0.051              | 1.135              | 7.836                                | 0.064                      |
| d-aug-cc-pVDZ | CCSD             | 1.370                    | 2.945                                | 0.049              | 1.119              | 7.787                                | 0.063                      |
|               | CCSDT            | 1.432                    | 2.927                                | 0.049              | 1.096              | 7.894                                | 0.055                      |
| d-aug-cc-pVTZ | CCSD             | 1.409                    | 2.900                                | 0.048              | 1.084              | 7.822                                | 0.054                      |
|               | CCSDT            | 1.440                    | 2.918                                | 0.050              | 1.111              | 7.949                                | 0.050                      |
| d-aug-cc-pVQZ | CCSD             | 1.416                    | 2.890                                | 0.048              | 1.098              | 7.876                                | 0.050                      |
|               | CCSDT            | 1.409                    | 2.901                                | 0.048              | 1.084              | 7.837                                | 0.055                      |
| aug-cc-pVTZ   | TBE <sup>b</sup> | 1.42 ± 0.00              | 2.88 ± 0.01                          | 0.048 ± 0.001      | 1.11 ± 0.01        | 7.91 ± 0.01                          | 0.046 ± 0.001              |
| CBS           | TBE <sup>c</sup> | 1.425 <sup>d</sup>       | 2.944 <sup>e</sup>                   |                    | 1.106 <sup>g</sup> | 7.94 <sup>h</sup>                    | 0.081 <sup>h</sup>         |
| lit.          | th.              |                          |                                      |                    |                    |                                      | 0.051 <sup>k</sup>         |
|               | exp.             | 1.27 ± 0.21 <sup>i</sup> |                                      | 0.044 <sup>j</sup> |                    | 8.05 <sup>k</sup>                    |                            |
|               |                  |                          |                                      |                    |                    |                                      | 0.042 ± 0.004 <sup>l</sup> |
|               |                  |                          |                                      |                    |                    |                                      | 0.052 ± 0.006 <sup>m</sup> |

<sup>a</sup>Transition energies are in eV and dipoles in D. <sup>b</sup>Computed using CCSDTQ/aug-cc-pVTZ values and CCSDTQP/aug-cc-pVDZ corrections. Note that CCSDTQ is equivalent to FCI for BH. <sup>c</sup>See the Computational Methods section. <sup>d</sup>Average between the MR-ACPF/aug-cc-pCV7Z(i) values obtained for  $r = 1.220$  and  $1.225$  Å in ref 90. <sup>e</sup>FCI/aug-cc-pVDZ value of ref 54. <sup>f</sup>CC2/aug-cc-pVQZ result from ref 45. <sup>g</sup>CCSD(T)/CBS value from ref 47. <sup>h</sup>CISDTQ/aug-cc-pCVQZ value from ref 91. A  $f$  value of 0.071 is also reported in Table 2 of the same work. <sup>i</sup>Stark (emission) measurements of ref 92. <sup>j</sup> $f_{00}$  obtained from laser-induced fluorescence in ref 93. There are no major contributions from other bands according to this work (see references therein for previous experimental values). A slightly older experiment (ref 94) reports a smaller estimate of  $0.045 \pm 0.02$ . <sup>k</sup>Absorption values from ref 95 ( $\Delta E$  corresponds to the maximum of absorption). <sup>l</sup>EELS value from ref 96. <sup>m</sup>HR-EELS value from ref 97.

DFT) is obviously natural, but such a task is difficult because of the lack of definite reference values. In this framework, we also note some very recent efforts for computing ES first-order properties with the many-body expansion FCI approach.<sup>52</sup>

## 2. COMPUTATIONAL METHODS

**2.1. Geometries and Basis Sets.** All our geometries are obtained at the CC3/aug-cc-pVTZ<sup>53,54</sup> level without using the frozen-core (FC) approximation (*i.e.*, we correlate all the electrons). These geometries are given in the [Supporting Information](#). Note that several structures come from previous studies,<sup>5,8</sup> and we used this level of theory here for consistency. New optimizations have been achieved with the DALTON 2017<sup>55</sup> and CFOUR 2.1<sup>56</sup> codes, applying default parameters in both cases.

As in our previous studies,<sup>5–8</sup> we consider the diffuse-containing Pople's 6-31+G(d) and Dunning's (d)-aug-cc-pVXZ ( $X = D, T, Q,$  and  $5$ ) atomic basis sets in all ES calculations.

In contrast with our previous studies, in which the complete basis set limit (CBS) could be obtained by a brute-force approach,  $f$  and  $\mu^{\text{ES}}$  converge, in some cases, slower than the energy with respect to the basis set size. Therefore, we have performed CBS extrapolation by applying the well-known Helgaker formula<sup>57</sup>

$$P_{\text{CBS}} = \frac{P_{X-1}(X-1)^3 - P_X X^3}{(X-1)^3 - X^3} \quad (1)$$

in which  $X$  equals 2, 3, 4, ... for D, T, Q, ... in the Dunning series and  $P$  is the property under investigation. Interestingly, this approach was successfully used for GS dipole moments.<sup>58</sup> In practice, we performed four extrapolations using both the CCSD and CCSDT results obtained with the pairs of largest singly- and doubly augmented basis sets accessible of at least triple- $\zeta$  size, that is, (i) CCSD/aug-cc-pVQZ and aug-cc-pV5Z; CCSDT/aug-cc-pVTZ and aug-cc-pVQZ; CCSD/d-aug-cc-pVTZ and d-aug-cc-pVQZ; and CCSDT/d-aug-cc-pVTZ and d-aug-cc-pVQZ for molecules in [Sections 3.1–3.5](#) and (ii) CCSD/aug-cc-pVTZ and aug-cc-pVQZ; and CCSD/d-aug-cc-pVTZ and d-aug-cc-pVQZ for molecules in [Sections 3.6–3.9](#). In such a way, we can estimate the extrapolation error and provide error bars for the CBS values, although such an error bar is likely underestimated for the latter set of compounds. These CCSD and/or CCSDT CBS values are next used to correct the properties obtained at higher levels (*e.g.*, CCSDTQ) with a finite basis using the approach described below.

**2.2. Reference Calculations.** We have chosen to use the MRCC (2017 and 2019) program<sup>59,60</sup> for performing our CC calculations, as this code allows us to set up an arbitrary CC expansion order. We therefore use the CCSD,<sup>61–65</sup> CCSDT,<sup>66–70</sup> CCSDTQ,<sup>71–74</sup> and CCSDTQP<sup>72–74</sup> hierarchy for energies, oscillator strengths, and GS and ES dipoles, respectively. All these values have been obtained within the FC approximation. The interested reader may find discussions about the impact of this approximation and the importance of core correlation functions for transition energies in some of our previous studies.<sup>22,75</sup> For CCSD, we performed several test calculations with GAUSSIAN 16,<sup>76</sup> Q-CHEM 5.2,<sup>77</sup> DALTON 2017,<sup>55</sup> and  $e^T$  1.0,<sup>78</sup> and we could not detect any significant discrepancy with respect to the MRCC results. At this stage, it is important to stress that all these calculations rely on the so-

called linear-response (LR) formalism,<sup>73,79,80</sup> such that while the same transition energies would be obtained with the equation-of-motion (EOM) approach, the properties would be different. However, it is known that the two formalisms become equivalent when the CC wave function becomes exact. As we strive here to be as close as possible from the FCI limit, we trust that our theoretical best estimates (TBEs) are not significantly affected by the selection of the LR implementation. At the CCSD level, we also provide a comparison between the EOM and LR oscillator strength values obtained with various codes in Table S1 in the [Supporting Information](#). The differences found between the EOM and LR formalisms are very small. The interested reader may also find extensive comparisons of oscillator strengths determined within the two formalisms elsewhere.<sup>81</sup> We also note that all our oscillator strengths are given in the length gauge, the most commonly applied gauge, but again, this choice is likely irrelevant when one is targeting near-exact values. The interested reader can find comparisons between CC oscillator strengths determined with the length, velocity, and mixed length-velocity gauges on small compounds elsewhere.<sup>82</sup> As expected, the impact of the gauge was found to decrease when increasing the order of the CC expansion, especially when triples are included. Finally, we report in the tables below, the so-called orbital-relaxed dipoles, which are more accurate than the so-called orbital-unrelaxed dipoles in which the impact of the external field on the orbitals is neglected. Details on various approaches and their implementations for correlated first-order properties can be found elsewhere.<sup>80,83,84</sup>

Beyond the basis set extrapolation discussed above, we also define TBEs in the following. To this end, we use an incremental strategy for the transition energies and dipoles, for example, at the aug-cc-pVTZ level

$$P(\text{TBE}) = P(\text{low/AVTZ}) + P(\text{high/AVDZ}) - P(\text{low/AVDZ}) \quad (2)$$

$$f(\text{TBE}) = f(\text{low/AVTZ}) \frac{f(\text{high/AVDZ})}{f(\text{low/AVDZ})} \quad (3)$$

where low and high denote, for example, CCSDTQ and CCSDTQP (see footnotes in the tables for specific details). For oscillator strengths, we applied the corresponding multiplicative approach, for example

Such an incremental strategy that used a double- $\zeta$  result to estimate "Q" or "P" effects is commonly employed in the CC literature.<sup>73,85–89</sup>

## 3. RESULTS AND DISCUSSION

Below, we discuss individual molecules going up on size progressively. Concerning literature references, we do not intend to provide an exhaustive list of all previous studies for each system considered here, but rather to highlight the studies and comparisons that we have found valuable for the present work.

**3.1. BH and HCl.** Let us start by a tiny compound, BH. Our results are listed in [Table 1](#), and although the size of this molecule seems ridiculous (only 4 valence electrons), some valuable conclusions can be obtained. We note that  $\mu^{\text{GS}}$  is slightly too large with CCSD (irrespective of the basis set) but the CC convergence is fast and CCSDT is obviously sufficient. Our TBE/CBS of 1.42 D for  $\mu^{\text{GS}}$  is equivalent to a recent ultra-accurate estimate<sup>90</sup> and also falls within the error bar of the

Table 2. GS Dipole Moment  $\mu^{\text{GS}}$ , Vertical Transition Energies  $\Delta E_{\text{vert}}$ , Oscillator Strengths  $f$ , and ES Dipole Moments  $\mu_{\text{vert}}^{\text{ES}}$  Determined for H<sub>2</sub>O (GS Geometry)<sup>a</sup>

| basis         | method           | <sup>1</sup> A <sub>1</sub> ( $\mu^{\text{GS}}$ ) |                          | <sup>1</sup> B <sub>1</sub> (Ryd, n → 3s) |                                 | <sup>1</sup> A <sub>2</sub> (Ryd, n → 3p) |                                 | <sup>1</sup> A <sub>1</sub> (Ryd, n → 3s) |                    |
|---------------|------------------|---|--------------------------|---|---------------------------------|---|---------------------------------|---|--------------------|
|               |                  | $\mu^{\text{GS}}$                                 | $\Delta E_{\text{vert}}$ | $f$                                       | $\mu_{\text{vert}}^{\text{ES}}$ | $\Delta E_{\text{vert}}$                  | $\mu_{\text{vert}}^{\text{ES}}$ | $\Delta E_{\text{vert}}$                  | $f$                |
| aug-cc-pVDZ   | CCSD             | 1.870   | 7.447                    | 0.057                                     | -1.404                          | 9.213                                     | -0.936                          | 9.861                                     | 0.103              |
|               | CCSDT            | 1.849   | 7.497                    | 0.058                                     | -1.420                          | 9.279                                     | -0.978                          | 9.903                                     | 0.104              |
|               | CCSDTQ           | 1.848   | 7.529                    | 0.058                                     | -1.415                          | 9.313                                     | -0.974                          | 9.937                                     | 0.105              |
|               | CCSDTQP          | 1.848   | 7.522                    | 0.058                                     | -1.414                          | 9.318                                     | -0.972                          | 9.941                                     | 0.105              |
| aug-cc-pVTZ   | CCSD             | 1.864   | 7.597                    | 0.053                                     | -1.549                          | 9.361                                     | -1.056                          | 9.957                                     | 0.098              |
|               | CCSDT            | 1.842   | 7.591                    | 0.054                                     | -1.565                          | 9.368                                     | -1.110                          | 9.949                                     | 0.100              |
|               | CCSDTQ           | 1.840   | 7.620                    | 0.054                                     | -1.559                          | 9.401                                     | -1.107                          | 9.981                                     | 0.100              |
|               | CCSDT            | 1.873   | 7.660                    | 0.052                                     | -1.655                          | 9.422                                     | -1.237                          | 10.004                                    | 0.095              |
| aug-cc-pVQZ   | CCSDT            | 1.850   | 7.637                    | 0.053                                     | -1.667                          | 9.410                                     | -1.294                          | 9.980                                     | 0.097              |
|               | CCSD             | 1.876   | 7.683                    | 0.051                                     | -1.726                          | 9.444                                     | -1.309                          | 10.010                                    | 0.089              |
|               | CCSD             | 1.861   | 7.429                    | 0.052                                     | -1.759                          | 9.179                                     | -1.658                          | 9.731                                     | 0.050              |
|               | CCSDT            | 1.841   | 7.479                    | 0.053                                     | -1.754                          | 9.244                                     | -1.703                          | 9.792                                     | 0.057              |
| d-aug-cc-pVTZ | CCSD             | 1.865   | 7.592                    | 0.051                                     | -1.764                          | 9.348                                     | -1.626                          | 9.869                                     | 0.057              |
|               | CCSDT            | 1.843   | 7.586                    | 0.052                                     | -1.767                          | 9.353                                     | -1.681                          | 9.872                                     | 0.062              |
|               | CCSD             | 1.874   | 7.659                    | 0.051                                     | -1.765                          | 9.416                                     | -1.622                          | 9.932                                     | 0.058              |
|               | CCSDT            | 1.851   | 7.636                    | 0.052                                     | -1.770                          | 9.403                                     | -1.678                          | 9.917                                     | 0.063              |
| aug-cc-pVTZ   | TBE <sup>b</sup> | 1.840   | 7.614                    | 0.054                                     | -1.558                          | 9.405                                     | -1.106                          | 9.985                                     | 0.100              |
|               | TBE <sup>b</sup> | 1.86 ± 0.01                                       | 7.71 ± 0.02              | 0.052 ± 0.001                             | -1.77 ± 0.04                    | 9.49 ± 0.02                               | -1.67 ± 0.01                    | 9.99 ± 0.01                               | 0.062 ± 0.002      |
| CBS           | th.              | 1.853 <sup>c</sup>                                | 7.66 <sup>c</sup>        | 0.054 <sup>d</sup>                        | -1.787 <sup>c</sup>             | 9.42 <sup>c</sup>                         | -1.682 <sup>c</sup>             | 9.97 <sup>e</sup>                         | 0.100 <sup>d</sup> |
|               | exp.             | 1.850 <sup>b</sup>                                | 7.70 <sup>e</sup>        | 0.049 <sup>f</sup>                        | 7.71 <sup>f</sup>               | 9.47 <sup>e</sup>                         | 9.92 <sup>g</sup>               | 9.67 <sup>f</sup>                         | 0.055 <sup>g</sup> |
| lit.          | th.              | 1.853 <sup>c</sup>                                | 7.66 <sup>c</sup>        | 0.054 <sup>d</sup>                        | -1.787 <sup>c</sup>             | 9.42 <sup>c</sup>                         | -1.682 <sup>c</sup>             | 9.97 <sup>e</sup>                         | 0.100 <sup>d</sup> |
|               | exp.             | 1.850 <sup>b</sup>                                | 7.71 <sup>f</sup>        | 0.046 ± 0.007 <sup>f</sup>                | 7.41 <sup>f</sup>               | 9.20 <sup>f</sup>                         | 9.67 <sup>f</sup>               | 9.67 <sup>f</sup>                         | 0.051 <sup>k</sup> |

<sup>a</sup>See the caption of Table 1 for details. <sup>b</sup>See the corresponding footnotes in Table 1. <sup>c</sup>CASPT2/d-aug-cc-pVQZ values from ref 99. <sup>d</sup>LR-CC3/aug-cc-pVTZ value from ref 5. <sup>e</sup>Basis set corrected exFCI/aug-cc-pVQZ values from ref 5. <sup>f</sup>2FVCAS/MR-CI/CBS values ( $f$  in length gauge) from ref 48. <sup>g</sup>2FVCAS/MR-CI/d-aug-cc-pVQZ values ( $f$  in length gauge) from ref 100. <sup>h</sup>Average of the three (very close) experimental values reported in Table 1 of ref 101. <sup>i</sup>Energy loss experiment from ref 102. <sup>j</sup>Electron impact from ref 103. <sup>k</sup>Electron impact from ref 104 integrated by Borges in ref 100.

**Table 3.** GS Dipole Moment  $\mu^{\text{GS}}$ , Vertical Transition Energies  $\Delta E_{\text{vert}}$ , Oscillator Strengths  $f$ , and ES Dipole Moments  $\mu^{\text{ES}}$  Determined for H<sub>2</sub>S (GS Geometry)<sup>a</sup>

| basis         | method           | <sup>1</sup> A <sub>1</sub> | <sup>1</sup> A <sub>2</sub> (Ryd, n → 4p)                 |                    | <sup>1</sup> B <sub>1</sub> (Ryd, n → 4s)                 |   |                     |
|---------------|------------------|-----------------------------|---|--------------------|---|---|---------------------|
|               |                  | $\mu^{\text{GS}}$           | $\Delta E_{\text{vert}}$                                  | $\mu^{\text{ES}}$  | $\Delta E_{\text{vert}}$                                  | $f$                                       | $\mu^{\text{ES}}$   |
| aug-cc-pVDZ   | CCSD             | 1.031                       | 6.343   | 0.113              | 6.141   | 0.068                                     | -1.983              |
|               | CCSDT            | 1.016                       | 6.286   | 0.131              | 6.098   | 0.067                                     | -1.946              |
|               | CCSDTQ           | 1.015                       | 6.286   | 0.137              | 6.103   | 0.067                                     | -1.934              |
|               | CCSDTQP          | 1.015                       | 6.286   | 0.137              | 6.103   | 0.067                                     | -1.933              |
| aug-cc-pVTZ   | CCSD             | 0.990                       | 6.246   | 0.503              | 6.295   | 0.064                                     | -1.893              |
|               | CCSDT            | 0.978                       | 6.185   | 0.496              | 6.237   | 0.063                                     | -1.875              |
|               | CCSDTQ           | 0.977                       | 6.181   | 0.498              | 6.238   | 0.063                                     | -1.866              |
| aug-cc-pVQZ   | CCSD             | 1.001                       | 6.212   | 0.650              | 6.349   | 0.062                                     | -1.822              |
|               | CCSDT            | 0.990                       | 6.153   | 0.636              | 6.288   | 0.061                                     | -1.815              |
| aug-cc-pVSZ   | CCSD             | 0.998                       | 6.177   | 0.691              | 6.368   | 0.061                                     | -1.794              |
|               | CCSDT            | 0.998                       | 6.177   | 0.691              | 6.368   | 0.061                                     | -1.794              |
| d-aug-cc-pVDZ | CCSD             | 1.017                       | 6.297   | 0.445              | 6.130   | 0.065                                     | -1.811              |
|               | CCSDT            | 1.002                       | 6.241   | 0.458              | 6.086   | 0.065                                     | -1.776              |
| d-aug-cc-pVTZ | CCSD             | 0.989                       | 6.228   | 0.597              | 6.292   | 0.062                                     | -1.774              |
|               | CCSDT            | 0.977                       | 6.167   | 0.587              | 6.234   | 0.062                                     | -1.761              |
| d-aug-cc-pVQZ | CCSD             | 1.001                       | 6.206   | 0.668              | 6.347   | 0.061                                     | -1.758              |
|               | CCSDT            | 0.989                       | 6.147   | 0.653              | 6.286   | 0.061                                     | -1.755              |
| aug-cc-pVTZ   | TBE <sup>b</sup> | 0.977                       | 6.181   | 0.498              | 6.238   | 0.063                                     | -1.865              |
| CBS           | TBE <sup>b</sup> | 0.99 ± 0.01                 | 6.10 ± 0.03   | 0.72 ± 0.01        | 6.33 ± 0.01   | 0.060 ± 0.001                             | -1.74 ± 0.02        |
| lit.          | th.              | 0.989 <sup>c</sup>          | 6.12 <sup>c</sup> ; 6.10 <sup>d</sup> ; 6.10 <sup>e</sup> | 0.653 <sup>c</sup> | 6.27 <sup>c</sup> ; 6.29 <sup>d</sup> ; 6.33 <sup>e</sup> | 0.063 <sup>f</sup>                        | -1.733 <sup>c</sup> |
|               | exp.             | 0.974 ± 0.005 <sup>g</sup>  |   |                    | 6.326 <sup>h</sup>  | 0.0542 <sup>i</sup> ; 0.0547 <sup>j</sup> |                     |

<sup>a</sup>See the caption of Table 1 for details. <sup>b</sup>See the corresponding footnotes in Table 1. <sup>c</sup>CASPT2/d-aug-cc-pVQZ values from ref 99. <sup>d</sup>Basis set corrected exFCI/aug-cc-pVQZ values from ref 5. <sup>e</sup>SS-RASPT2/ANO-RCC-VTZP + diffuse values from ref 105. <sup>f</sup>LR-CC3/aug-cc-pVTZ value from ref 5. <sup>g</sup>From ref 106. <sup>h</sup>From ref 107 (see Table 9 of this work). <sup>i</sup>From ref 108, obtained by integrating the experimental absorption spectrum in the 5.2–7.7 eV region. <sup>j</sup>From ref 109, obtained by integrating the experimental absorption spectrum in the 5.2–7.7 eV region.

only available experimental value we are aware of:  $1.27 \pm 0.21$  D.<sup>92</sup> Such a large error bar is explainable: the experiment relied on an analysis of the emission spectrum.<sup>92</sup> It is quite obvious that the theoretical estimate is more trustworthy in this specific case, indicating that previous error analyses based on the 1.27 D value likely significantly exaggerated the ADC(2) and CC2 overestimations<sup>45</sup> but slightly underestimated the QMC error<sup>98</sup> for  $\mu^{\text{GS}}$ . For the lowest transition energy in BH, our values fit with previous FCI calculations,<sup>54</sup> and one again notices a rather quick convergence of  $\Delta E_{\text{vert}}$  with respect to both basis set size and CC order. For the oscillator strength, there is also an astonishing stability of the values, as the considered ES is well separated from higher-lying ones of the same spatial symmetry. Our TBE is close to the most recent measurement (of  $f_{00}$ ) we could find.<sup>93</sup> For  $\mu^{\text{ES}}$ , one notes a very small decrease in the amplitude between the GS and ES geometries, which is a logical consequence of the tiny geometrical relaxation (+0.018 Å), and our TBE is within the rather small experimental error bar (see bottom of Table 1). Finally, as can be seen in Table S2, these results are not affected by the FC approximation, for example, the difference between CCSDTQ(FC)/aug-cc-pVTZ and CCSDTQ(Full)/aug-cc-pCVTZ is 0.001 for  $f$  and 0.002 D for the dipole moments.

For HCl, the GS dipole moment does not cause any specific challenge and our TBE is equivalent to the one recently reported by the Head-Gordon group.<sup>47</sup> As expected,<sup>5</sup> CCSDTQ provides converged  $\Delta E_{\text{vert}}$  and this holds for both  $f$  and  $\mu^{\text{ES}}$ . When increasing the size of the basis set, one sees a significant decrease of the oscillator strength (*ca.* -25% from aug-cc-pVDZ to aug-cc-pVSZ) and of the ES dipole (-16% for the same basis pair), whereas the transition energy varies by 1% only. Nevertheless, the CBS extrapolations are stable for all

investigated properties. For HCl, it is difficult to obtain a very accurate experimental  $f$  value, in part because of the mixing of the <sup>1</sup>Π and <sup>3</sup>Π states.<sup>95</sup> There is therefore a broad range of measured values (see bottom of Table 1 as well as Table 2 in ref 97), and our TBE/CBS of 0.046 is compatible with the two most recent experiments. In contrast, we could not find any experimental  $\mu^{\text{ES}}$  estimate, which is a logical consequence of the dissociative character of the lowest singlet ES of HCl.

**3.2. H<sub>2</sub>O and H<sub>2</sub>S.** The results obtained for water and hydrogen sulfide are listed in Tables 2 and 3, respectively. The CCSDT/aug-cc-pVTZ estimate of the GS dipole of water is already within 0.01 D of both previous CASPT2<sup>99</sup> and experimental values.<sup>101</sup> For all transition energies, as discussed in our earlier work,<sup>5</sup> the calculations are converged with CCSDTQ, but one needs a rather large basis set (especially in terms of diffuse functions) to be chemically accurate, which is quite usual for Rydberg transitions in small compounds. Nevertheless, CCSDT/aug-cc-pVTZ delivers  $\Delta E_{\text{vert}}$  with an error of 1–3% only as compared to the most accurate estimates (see bottom of Table 2) for all three transitions. For the lowest B<sub>1</sub> excitation, the oscillator strength  $f$  varies rather mildly with the selected level of theory and basis set, although one notices a general decreasing trend when improving the method. Our TBE of  $0.052 \pm 0.001$  falls in the error bar of a recent experiment<sup>103</sup> and is only slightly larger than the previous most accurate TBE we are aware of.<sup>48</sup> More exhaustive lists of additional theoretical and experimental values or this oscillator strength can be found in Table 4 of ref 103 and Table 6 of ref 48 for the lowest transition. The reported  $f$  values in these tables are in the range 0.041–0.060. The magnitude of  $\mu^{\text{ES}}$  for this B<sub>1</sub> ES increases significantly with the basis set size, and a difference of -0.21 D exists between our aug-cc-pVTZ and CBS TBES. The latter compares well

**Table 4.** GS Dipole Moment  $\mu^{\text{GS}}$ , Vertical Transition Energies  $\Delta E_{\text{vert}}$ , Oscillator Strengths  $f$ , and ES Dipole Moments  $\mu^{\text{ES}}$  Determined for BF (GS Geometry)<sup>a</sup>

| basis         | method           | <sup>1</sup> A <sub>1</sub> | <sup>1</sup> Π(Val, σ → π*) |                   |                   |
|---------------|------------------|-----------------------------|-----------------------------|-------------------|-------------------|
|               |                  | $\mu^{\text{GS}}$           | $\Delta E_{\text{vert}}$    | $f$               | $\mu^{\text{ES}}$ |
| aug-cc-pVDZ   | CCSD             | 0.832                       | 6.534                       | 0.479             | 0.240             |
|               | CCSDT            | 0.861                       | 6.491                       | 0.475             | 0.311             |
|               | CCSDTQ           | 0.861                       | 6.486                       | 0.474             | 0.316             |
|               | CCSDTQP          | 0.860                       | 6.485                       | 0.474             | 0.316             |
| aug-cc-pVTZ   | CCSD             | 0.794                       | 6.464                       | 0.475             | 0.222             |
|               | CCSDT            | 0.824                       | 6.423                       | 0.469             | 0.293             |
|               | CCSDTQ           | 0.824                       | 6.417                       | 0.468             | 0.300             |
| aug-cc-pVQZ   | CCSD             | 0.783                       | 6.449                       | 0.475             | 0.207             |
|               | CCSDT            | 0.812                       | 6.411                       | 0.468             | 0.279             |
| aug-cc-pVSZ   | CCSD             | 0.782                       | 6.443                       | 0.475             | 0.202             |
|               | CCSD             | 0.822                       | 6.521                       | 0.478             | 0.262             |
| d-aug-cc-pVDZ | CCSDT            | 0.850                       | 6.477                       | 0.474             | 0.330             |
|               | CCSD             | 0.794                       | 6.459                       | 0.476             | 0.237             |
| d-aug-cc-pVTZ | CCSDT            | 0.824                       | 6.419                       | 0.469             | 0.308             |
|               | CCSD             | 0.784                       | 6.448                       | 0.475             | 0.213             |
| d-aug-cc-pVQZ | CCSDT            | 0.813                       | 6.409                       | 0.468             | 0.285             |
|               | CCSD             | 0.813                       | 6.409                       | 0.468             | 0.285             |
| aug-cc-pVTZ   | TBE <sup>b</sup> | 0.824                       | 6.417                       | 0.468             | 0.299             |
| CBS           | TBE <sup>b</sup> | 0.80 ± 0.01                 | 6.39 ± 0.01                 | 0.467 ± 0.001     | 0.27 ± 0.01       |
| lit.          | th.              | 0.84 <sup>c</sup>           | 6.329 <sup>d</sup>          | 0.30 <sup>e</sup> | 0.01 <sup>c</sup> |
|               | exp.             | 0.5 ± 0.2 <sup>f</sup>      |                             | 0.40 <sup>g</sup> |                   |

<sup>a</sup>See the caption of Table 1 for details. <sup>b</sup>See the corresponding footnotes in Table 1. <sup>c</sup>MRCI+Q/aug-cc-pV6Z values from ref 114, the ES dipole was obtained on the corresponding ES geometry. <sup>d</sup>CIPSI/(11s7p4d3f)/[6s4p4d3f] estimate from ref 115. <sup>e</sup>Sum of the MRCI  $f$  value determined for GS  $\nu'' = 0$ , from Table 5 of ref 113. <sup>f</sup>From ref 112. <sup>g</sup> $f_{00}$  value from ref 116.

with an earlier CASPT2 value.<sup>99</sup> This trend is even exacerbated for the  $\mu^{\text{ES}}$  value associated with the A<sub>2</sub> state that changes by −0.56 D from aug-cc-pVTZ to CBS, whereas no significant changes can be noticed between CCSDT and CCSDTQ. For the lowest A<sub>1</sub> ES, there is a significant mixing with a close-lying state of the same symmetry, and the addition of a second set of diffuse is mandatory to obtain reasonable estimates of the oscillator strength (which is much too large with aug-cc-pVTZ). Our TBE/CBS  $f$  value of 0.062 could still be slightly too large, but the available experimental values range from 0.041 to 0.073 (see Table 3 in ref 100). In contrast to what we found for the two lower-lying ESs,  $\mu^{\text{ES}}$  for the A<sub>1</sub> ES is not very sensitive to the basis set size, with a difference of −0.09 D only between the aug-cc-pVTZ and CBS TBES. We can already conclude, from the data of Table 2, that the basis set required to reach accurate estimates not only differs from one ES to another, but might also be very different, for a given ES, or the oscillator strengths and ES dipoles. On a brighter note, the improvements brought by the Q and P excitations are rather limited, meaning that CCSDT seems already sufficient (for water at least).

As can be seen in Table 3, the GS dipole moment of hydrogen sulfide remains almost unchanged when increasing the CC order or the size of the basis set: all estimates fall in a tight window: 1.00 ± 0.03 D. Our TBE/CBS of 0.99 D is very close from the experimental value of 0.974 ± 0.005 D, although we use a theoretical geometry. For the lowest <sup>1</sup>A<sub>2</sub> transition, the excitation energies are almost converged with CCSDT but a rather large basis set is required, like in water. Our TBE/CBS of 6.10 ± 0.03 eV agrees with previous high-order estimates.<sup>5,99,105</sup> To the best of our knowledge there are no accurate experimental estimates for this dark state. Although the methodological effects remain firmly under control for the ES dipole, CCSDT being again sufficient, the

basis set effects are huge: at the CCSDT level, we have  $\mu^{\text{ES}} = 0.13$  D with aug-cc-pVDZ but more than four times larger (0.65 D) with d-aug-cc-pVQZ. Our TBE/CBS of 0.72 ± 0.02 D is slightly larger than the best previous estimate we have found (0.65 D).<sup>99</sup> The transition energy to the second ES, of B<sub>1</sub> symmetry, is also basis set sensitive, although in that case larger bases yield larger (and not smaller) transition energies, as shown in Table 3. Our TBE/CBS of 6.33 ± 0.01 eV is close to previous estimates<sup>5,99,105</sup> and also consistent with measurements,<sup>107</sup> although we recall that such comparisons should be made with care. The dipole moment of the B<sub>1</sub> state is very large and relatively insensitive to the basis set as compared to its A<sub>2</sub> counterpart. Our TBE/CBS of −1.74 ± 0.02 D is very close to an earlier CASPT2 estimate.<sup>99</sup> Finally, the computed oscillator strength is rather methodologically insensitive and our best estimate of 0.060 is within 0.010 of the two most recent measurements we could find<sup>108,109</sup> and compares favorably with two (rather old) theoretical estimates: 0.081<sup>110</sup> and 0.075.<sup>111</sup>

**3.3. BF.** For this diatomic, the lowest Π ES behaves rather nicely, and one notices in Table 4 that we could reach very stable estimates for all investigated properties, CCSDT/aug-cc-pVTZ delivering already sufficiently accurate values. It is noteworthy that for any given basis set, CCSD underestimates  $\mu^{\text{GS}}$  ( $\mu^{\text{ES}}$ ) by ca. 4% (25%), highlighting the difficulty posed by ES for “simple” methods. The experimental value of  $\mu^{\text{GS}}$  was measured to be 0.5 ± 0.2 D,<sup>112</sup> a value that was suggested to be too low more than five scores ago.<sup>113</sup> Indeed, the present TBE/CBS of 0.80 D is significantly above the upper limit of the experimental error bar but in good agreement with an earlier MRCI+Q value (0.84 D) obtained with a very large basis set.<sup>114</sup> Our best estimate for  $\Delta E_{\text{vert}}$  6.39 eV, is slightly larger than a rather old CIPSI value of 6.329 eV,<sup>115</sup> whereas unfortunately, ref 114 lists adiabatic energies only. For the

oscillator strength, the TBE in Table 4 is larger than previous experimental<sup>116</sup> and theoretical<sup>113</sup> data, but the uniformity of our estimates gives confidence in their quality. Eventually, we predict a significant drop in polarity when going from the GS to the ES, with a  $\mu^{\text{ES}}$  value of *ca.* 0.27 D. This value is much larger than the MRCI+Q  $\mu^{\text{ES}}$  reported by Magoulas and co-workers (0.01 D),<sup>114</sup> but the latter is obtained on the ES rather than the GS geometry which might explain this apparent discrepancy.

**3.4. CO.** For C=O, we considered six different ESs of various nature, and our results are listed in Table 5. For the three lowest transitions of valence character, one notices that CCSDT is again sufficient, with very small corrections brought by the Q and P excitations, for example, the Q-induced changes attain *ca.*  $\pm 0.01$ – $0.02$  D only for  $\mu^{\text{ES}}$ . For these three transitions, the basis set effects are also firmly under control for all properties, and, both  $f$  and  $\mu^{\text{ES}}$  are not significantly affected by the second set of diffuse orbitals, and aug-cc-pVQZ is likely sufficiently large to obtain accurate estimates. As a consequence, it is rather straightforward to obtain stable CBS extrapolations. The moderate impact brought by the quadruples seems to pertain for the three higher-lying Rydberg ESs of carbon monoxide, except for the dipole moment of the second  $^1\Sigma^+$  transition for which  $\mu^{\text{ES}}$  increases by +0.111 D when going from CCSDT/aug-cc-pVTZ to CCSDTQ/aug-cc-pVTZ. As expected, much larger basis sets are needed to obtain converged properties for the Rydberg ESs than for their valence counterparts. Indeed, when going from aug-cc-pVTZ to d-aug-cc-pVQZ, the CCSDT ES dipoles of the three lowest Rydberg states drastically change from  $-3.89$  to  $-1.81$  D, from  $+6.09$  to  $+4.34$  D, and from  $+0.14$  to  $-1.44$  D, respectively. In the same time, the CCSDT value of  $f$  for the two significantly dipole-allowed transitions decreases by  $\sim 36\%$  when considering the same basis set pair. Obviously such a behavior makes the error bar obtained for our TBE/CBS estimates non-negligible (see below). In contrast, and as already noted above, the transition energies of these Rydberg ESs can be effectively estimated with high accuracy.

When comparing with previously reported experimental and theoretical estimates, one should keep in mind that the properties of carbon monoxide are strongly affected by the bond length<sup>118</sup> and that we used a theoretical geometry with a slightly too elongated double bond (2.142 *vs* 2.132 bohr experimentally). Our TBE/CBS for  $\mu^{\text{GS}}$  is 0.10 D, which is slightly too low as compared to both the experimental measurement<sup>116</sup> and the theoretical calculations performed at the experimental geometry.<sup>47,123</sup> For the lowest and well-studied  $\Pi$  ES, the present  $8.46 \pm 0.01$  eV  $\Delta E_{\text{vert}}$  value is close to our recent FCI estimate (8.48 eV)<sup>5</sup> and to the experimental value (8.51 eV) deduced with the help of the measured spectroscopic constants and the reconstruction of the potential energy surface.<sup>124</sup> The computed value of  $f = 0.165$  is in very reasonable agreement with the estimates obtained by dipole ( $e, e$ ) and ( $\gamma, \gamma$ ) spectroscopies: 0.181<sup>119</sup> and 0.194,<sup>121</sup> respectively. We refer the interested readers to Tables 3 and 4 of ref 119, Table 6 of ref 125, and Table 2 of ref 126 for more complete lists of experimental and theoretical estimates of the oscillator strength for this state. There is a quite significant elongation of the double bond in the lowest ES. As a consequence, the value of  $\mu^{\text{ES}}$  determined on the GS ( $-0.19 \pm 0.01$  D) and ES ( $-0.39 \pm 0.01$  D) structures does differ significantly. The two Stark effect measurements we are aware of yield  $\mu^{\text{ES}} = -0.15 \pm 0.05$  D (analysis of the 0–0 band)<sup>120</sup>

and  $\mu^{\text{ES}} = -0.34 \pm 0.01$  D (two-photon LIF),<sup>122</sup> which are also somehow inconsistent, yet of the same order of magnitude as our GS and ES values, respectively. For the two other valence transitions, of  $\Sigma^-$  and  $\Delta$  symmetries, the TBE/CBS for  $\Delta E_{\text{vert}}$  shows small errors (1–2%) as compared to the “experimental” values.<sup>49</sup> We could not find any experimental estimate of the ES dipoles for these states, likely because they are dark, and we believe that the data listed in Table 5 stand as the most accurate ES dipole values proposed to date. They indicate that the dipole moments of these two ESs are parallel to the one of the GSs but have much larger amplitudes. For the three Rydberg transitions considered, our best estimates of the transition energies are fully compatible with the measurements. The lowest Rydberg ES has a very low oscillator strength, a result consistent with previous theoretical<sup>5,49</sup> and experimental<sup>119</sup> investigations. More interestingly, its dipole moment is large and negative. The two available measurements return dipoles of  $-1.60 \pm 0.15$ <sup>120</sup> and  $-1.95 \pm 0.03$  D,<sup>122</sup> whereas the strong basis set effects bring uncertainty to our TBE/CBS ( $-2.49 \pm 0.59$  D). The lower bound ( $-1.90$  D) fits the latest experimental value quite well. We have also computed the ES dipole of this state at its equilibrium geometry, but the changes are very limited (see Table S4 in the Supporting Information). The second Rydberg  $\Sigma^+$  transition is much more dipole-allowed than the first, and our TBE/CBS of  $0.146 \pm 0.016$  for the oscillator strength is consistent with the most recent measurement (0.136).<sup>121</sup> The dipole moment of this ES is large, positive, and rather unaffected by structural relaxation effects (Table S4 in the Supporting Information), our extrapolated value of  $4.94 \pm 0.47$  D agreeing well with the two available experimental estimates:  $4.52 \pm 0.35$ <sup>120</sup> and  $4.50 \pm 0.07$  D.<sup>122</sup> Eventually, for the highest ES of CO considered herein, the extrapolated  $f$  value perfectly fits the measurements.<sup>119,121</sup> We provide, as far as we know, the first estimate of its dipole moment, which is rather small and negative (see bottom of Table 5).

**3.5. N<sub>2</sub>.** The understanding of the nature of the ESs in the highly symmetric N<sub>2</sub> molecule is certainly challenging from both an experimental and theoretical points of view.<sup>127,128,130</sup> Of particular relevance for the present work is the nature and relative ordering of the three lowest  $^1\Pi_u$  states. Here, we have classified them following the nature of the underlying MOs<sup>132</sup> and characterized all of them as Rydberg, although alternative yet reasonable assignments can be found in the literature (*e.g.*, see Tables 1 and 2 in ref 128). Our results are given in Table 6. The convergence with respect to the CC excitation order is rather quick for both energies and oscillator strengths, with nevertheless non-negligible contributions from the quadruples for the transition energies, a likely consequence of the presence of a triple bond. If basis set effects follow the expected trends for the energies of these high-lying ESs (*i.e.*, a decrease in  $\Delta E_{\text{vert}}$  when increasing the basis set size and a significant impact of the second set of diffuse functions), the changes in the oscillator strength of the  $^1\Pi_u$  states when enlarging the basis set are dramatic. As an illustration, the oscillator strength of the second  $^1\Pi_u$  transition is 0.000 at the CCSDT/aug-cc-pVQZ level but 0.460 at the CCSDT/d-aug-cc-pVQZ level. If the extreme sensitivity of N<sub>2</sub>'s oscillator strengths to the computational setup is known for years (*e.g.*, see Table 6 in ref 127), it remains a very striking example of the state-mixing nightmare. As a consequence, while we could obtain solid TBE/aug-cc-pVTZ values in all cases, the extrapolation to CBS of the  $f$  values of the  $^1\Pi_u$  transitions is clearly problematic. In



Table 5. GS Dipole Moment  $\mu^{GS}$ , Vertical Transition Energies  $\Delta E_{\text{vert}}$ , Oscillator Strengths  $f$ , and ES Dipole Moments,  $\mu_{\text{vert}}^{\text{ES}}$  and  $\mu_{\text{adia}}^{\text{ES}}$  Determined for Various Transitions in CO at Its GS Geometry<sup>a</sup>

| basis         | method           | ${}^1\Sigma^+$           |                          |                                 | ${}^1\Pi(\text{Val}, n \rightarrow \pi^*)$ |   |                                 | ${}^1\Sigma^-(\text{Val}, \pi \rightarrow \pi^*)$ |                          |                                 | ${}^1\Delta(\text{Val}, \pi \rightarrow \pi^*)$ |                                 |                          |
|---------------|------------------|--------------------------|--------------------------|---------------------------------|--|---|---------------------------------|---|--------------------------|---------------------------------|---|---------------------------------|--------------------------|
|               |                  | $\mu^{GS}$               | $\Delta E_{\text{vert}}$ | $f$                             | $\mu_{\text{vert}}^{\text{ES}}$            | $\mu_{\text{adia}}^{\text{ES}}$         | $\Delta E_{\text{vert}}$        | $\mu_{\text{vert}}^{\text{ES}}$                   | $\Delta E_{\text{vert}}$ | $\mu_{\text{vert}}^{\text{ES}}$ | $\Delta E_{\text{vert}}$                        | $\mu_{\text{vert}}^{\text{ES}}$ | $\Delta E_{\text{vert}}$ |
| aug-cc-pVDZ   | CCSD             | 0.078                    | 8.671                    | 0.167                           | -0.157                                     | -0.438                                  | 10.096                          | 1.574   | 10.210                   | 1.405                           |   |                                 |                          |
|               | CCSDT            | 0.121                    | 8.574                    | 0.173                           | -0.079                                     | -0.331                                  | 10.062                          | 1.597   | 10.178                   | 1.432                           |   |                                 |                          |
|               | CCSDTQ           | 0.130                    | 8.563                    | 0.174                           | -0.072                                     | -0.317                                  | 10.057                          | 1.613   | 10.169                   | 1.446                           |   |                                 |                          |
|               | CCSDTQP          | 0.132                    | 8.561                    | 0.175                           | -0.069                                     | -0.312                                  | 10.057                          | 1.615   | 10.168                   | 1.448                           |   |                                 |                          |
|               | CCSD             | 0.051                    | 8.587                    | 0.161                           | -0.227                                     | -0.478                                  | 9.986                           | 1.577   | 10.123                   | 1.413                           |   |                                 |                          |
|               | CCSDT            | 0.104                    | 8.492                    | 0.164                           | -0.137                                     | -0.358                                  | 9.940                           | 1.595   | 10.076                   | 1.432                           |   |                                 |                          |
| aug-cc-pVQZ   | CCSDTQ           | 0.113                    | 8.480                    | 0.166                           | -0.129                                     | -0.344                                  | 9.932                           | 1.612   | 10.066                   | 1.449                           |   |                                 |                          |
|               | CCSD             | 0.039                    | 8.574                    | 0.160                           | -0.264                                     | -0.511                                  | 9.992                           | 1.567   | 10.127                   | 1.402                           |   |                                 |                          |
|               | CCSDT            | 0.094                    | 8.480                    | 0.163                           | -0.169                                     | -0.385                                  | 9.940                           | 1.586   | 10.073                   | 1.421                           |   |                                 |                          |
|               | CCSD             | 0.037                    | 8.571                    | 0.160                           | -0.280                                     | -0.523                                  | 10.087                          | 1.561   | 10.130                   | 1.398                           |   |                                 |                          |
|               | CCSD             | 0.085                    | 8.663                    | 0.167                           | -0.149                                     | -0.442                                  | 10.053                          | 1.584   | 10.167                   | 1.413                           |   |                                 |                          |
|               | CCSDT            | 0.128                    | 8.565                    | 0.173                           | -0.069                                     | -0.334                                  | 9.983                           | 1.568   | 10.120                   | 1.401                           |   |                                 |                          |
| d-aug-cc-pVTZ | CCSD             | 0.053                    | 8.582                    | 0.160                           | -0.232                                     | -0.483                                  | 9.937                           | 1.586   | 10.073                   | 1.421                           |   |                                 |                          |
|               | CCSDT            | 0.106                    | 8.487                    | 0.164                           | -0.141                                     | -0.364                                  | 9.992                           | 1.563   | 10.126                   | 1.397                           |   |                                 |                          |
|               | CCSD             | 0.040                    | 8.572                    | 0.160                           | -0.269                                     | -0.513                                  | 9.940                           | 1.581   | 10.073                   | 1.416                           |   |                                 |                          |
|               | CCSDT            | 0.094                    | 8.478                    | 0.163                           | -0.173                                     | -0.389                                  | 9.932                           | 1.614   | 10.065                   | 1.450                           |   |                                 |                          |
|               | TBE <sup>b</sup> | 0.115                    | 8.478                    | 0.166                           | -0.126                                     | -0.339                                  | 9.94 ± 0.01                     | 1.60 ± 0.01                                       | 10.07 ± 0.01             | 1.43 ± 0.01                     |   |                                 |                          |
|               | TBE <sup>b</sup> | 0.097 ± 0.002            | 8.46 ± 0.01              | 0.165 ± 0.001                   | -0.19 ± 0.01                               | -0.39 ± 0.01                            | 10.045 <sup>d</sup>             | 1.60 ± 0.01                                       | 10.182 <sup>d</sup>      | 1.43 ± 0.01                     |   |                                 |                          |
| lit.          | th.              | 0.1172 <sup>c</sup>      | 8.541 <sup>d</sup>       | 0.121 <sup>e</sup>              | -0.135 <sup>f</sup>                        | -0.05 <sup>h</sup> ; -0.19 <sup>f</sup> | 9.98 <sup>g</sup>               | 10.10 <sup>g</sup>                                | 10.10 <sup>g</sup>       | 1.43 ± 0.01                     |   |                                 |                          |
|               | exp.             | 0.091 <sup>f</sup>       | 8.48 <sup>g</sup>        | 0.168 <sup>g</sup>              | -0.181 <sup>i</sup>                        | -0.15 ± 0.05 <sup>m</sup>               | 9.88 <sup>k</sup>               | 10.25 <sup>k</sup>                                | 10.25 <sup>k</sup>       | 1.43 ± 0.01                     |   |                                 |                          |
|               | exp.             | 0.122 <sup>j</sup>       | 8.51 <sup>k</sup>        | 0.181 <sup>i</sup>              | 0.194 <sup>n</sup>                         | -0.335 ± 0.013 <sup>o</sup>             |                                 |   |                          |                                 |   |                                 |                          |
| basis         | method           | ${}^1\Sigma^+$ (Ryd)     |                          |                                 | ${}^1\Sigma^+$ (Ryd)                       |   |                                 | ${}^1\Pi$ (Ryd)                                   |                          |                                 |   |                                 |                          |
|               |                  | $\Delta E_{\text{vert}}$ | $f$                      | $\mu_{\text{vert}}^{\text{ES}}$ | $\Delta E_{\text{vert}}$                   | $f$                                     | $\mu_{\text{vert}}^{\text{ES}}$ | $\Delta E_{\text{vert}}$                          | $f$                      | $\mu_{\text{vert}}^{\text{ES}}$ |   |                                 |                          |
| aug-cc-pVDZ   | CCSD             | 11.171                   | 0.003                    | -4.134                          | 11.710                                     | 0.248                                   | 6.323                           | 11.973  | 0.132                    | 0.192                           |   |                                 |                          |
|               | CCSDT            | 10.944                   | 0.001                    | -4.519                          | 11.518                                     | 0.240                                   | 6.699                           | 11.767  | 0.124                    | 0.149                           |   |                                 |                          |
|               | CCSDTQ           | 10.926                   | 0.000                    | -4.572                          | 11.510                                     | 0.238                                   | 6.768                           | 11.758  | 0.122                    | 0.143                           |   |                                 |                          |
|               | CCSDTQP          | 10.919                   | 0.000                    | -4.592                          | 11.506                                     | 0.238                                   | 6.792                           | 11.753  | 0.121                    | 0.141                           |   |                                 |                          |
|               | CCSD             | 11.222                   | 0.008                    | -3.376                          | 11.751                                     | 0.208                                   | 5.600                           | 11.960  | 0.115                    | 0.195                           |   |                                 |                          |
|               | CCSDT            | 10.987                   | 0.004                    | -3.894                          | 11.540                                     | 0.203                                   | 6.094                           | 11.737  | 0.110                    | 0.138                           |   |                                 |                          |
| aug-cc-pVQZ   | CCSDTQ           | 10.963                   | 0.003                    | -3.994                          | 11.523                                     | 0.202                                   | 6.205                           | 11.720  | 0.108                    | 0.126                           |   |                                 |                          |
|               | CCSD             | 11.190                   | 0.010                    | -2.792                          | 11.733                                     | 0.183                                   | 5.097                           | 11.916  | 0.103                    | 0.084                           |   |                                 |                          |
|               | CCSDT            | 10.954                   | 0.006                    | -3.350                          | 11.514                                     | 0.180                                   | 5.619                           | 11.687  | 0.098                    | 0.007                           |   |                                 |                          |
|               | CCSD             | 11.133                   | 0.012                    | -2.077                          | 11.691                                     | 0.160                                   | 4.614                           | 11.851  | 0.091                    | -0.158                          |   |                                 |                          |
|               | CCSD             | 10.795                   | 0.009                    | -1.462                          | 11.393                                     | 0.134                                   | 3.498                           | 11.535  | 0.067                    | -1.957                          |   |                                 |                          |
|               | CCSDT            | 10.569                   | 0.006                    | -1.981                          | 11.175                                     | 0.129                                   | 3.927                           | 11.313  | 0.061                    | -2.146                          |   |                                 |                          |
| d-aug-cc-pVTZ | CCSD             | 10.960                   | 0.010                    | -1.337                          | 11.567                                     | 0.134                                   | 3.814                           | 11.700  | 0.074                    | -1.449                          |   |                                 |                          |
|               | CCSDT            | 10.726                   | 0.007                    | -1.855                          | 11.340                                     | 0.130                                   | 4.216                           | 11.468  | 0.069                    | -1.648                          |   |                                 |                          |
|               | CCSD             | 11.010                   | 0.011                    | -1.298                          | 11.617                                     | 0.134                                   | 3.946                           | 11.749  | 0.075                    | -1.233                          |   |                                 |                          |
|               | CCSDT            | 10.774                   | 0.007                    | -1.810                          | 11.388                                     | 0.130                                   | 4.337                           | 11.516  | 0.070                    | -1.437                          |   |                                 |                          |

Table S. continued

| basis       | method           | $^1\Sigma^+$ (Ryd)       |                    |                                 | $^1\Sigma^+$ (Ryd)       |                    |                                 | $^1\Pi$ (Ryd)            |                    |                                 |
|-------------|------------------|--------------------------|--------------------|---------------------------------|--------------------------|--------------------|---------------------------------|--------------------------|--------------------|---------------------------------|
|             |                  | $\Delta E_{\text{vert}}$ | $f$                | $\mu_{\text{vert}}^{\text{ES}}$ | $\Delta E_{\text{vert}}$ | $f$                | $\mu_{\text{vert}}^{\text{ES}}$ | $\Delta E_{\text{vert}}$ | $f$                | $\mu_{\text{vert}}^{\text{ES}}$ |
| aug-cc-pVTZ | TBE <sup>b</sup> | 10.956                   | 0.003              | -4.014                          | 11.519                   | 0.202              | 6.229                           | 11.715                   | 0.107              | 0.124                           |
| CBS         | TBE <sup>b</sup> | 10.84 ± 0.06             | 0.005 ± 0.001      | -2.49 ± 0.59                    | 11.43 ± 0.04             | 0.146 ± 0.016      | 4.94 ± 0.47                     | 11.58 ± 0.05             | 0.078 ± 0.009      | -0.70 ± 0.60                    |
| lit.        | th.              | 10.983 <sup>d</sup>      | 0.029 <sup>e</sup> | -2.79 <sup>f</sup>              |                          | 0.133 <sup>e</sup> | 5.34 <sup>f</sup>               |                          |                    |                                 |
|             |                  | 10.80 <sup>g</sup>       | 0.003 <sup>g</sup> |                                 | 11.42 <sup>g</sup>       | 0.200 <sup>g</sup> |                                 | 11.55 <sup>g</sup>       | 0.106 <sup>g</sup> |                                 |
| exp.        |                  | 10.78 <sup>k</sup>       | 0.009 <sup>l</sup> | -1.60 ± 0.15 <sup>m</sup>       | 11.40 <sup>k</sup>       | 0.121 <sup>l</sup> | 4.52 ± 0.35 <sup>m</sup>        | 11.53 <sup>k</sup>       | 0.074 <sup>l</sup> |                                 |
|             |                  |                          |                    | -1.95 ± 0.03 <sup>n</sup>       |                          | 0.136 <sup>n</sup> | 4.50 ± 0.07 <sup>o</sup>        |                          | 0.074 <sup>n</sup> |                                 |

<sup>a</sup>The transition energies are in eV and the dipoles are in D. <sup>b</sup>See the corresponding footnotes in Table 1. <sup>c</sup>CCSD(T)/CBS value from ref 47. <sup>d</sup>CCSDT/PVTZ + values from ref 68. <sup>e</sup>SOPPA (with "all corrections") from ref 49. <sup>f</sup>FCI/cc-pVDZ from ref 117. <sup>g</sup>From ref 5; the values of  $\Delta E_{\text{vert}}$  are basis set-corrected exFCI/aug-cc-pVQZ values, whereas  $f$  values are LR-CC3/aug-cc-pVTZ values. Note that a factor of two linked to the degeneracy was incorrectly omitted in this earlier work for the oscillator strengths of the two  $\Pi$  transitions. <sup>h</sup>CC2/AVQZ result from ref 45. <sup>i</sup>From ref 118. <sup>j</sup>From ref 116. <sup>k</sup>Vertical values estimated in ref 49 on the basis of the experimental spectroscopic data of ref 116. <sup>l</sup>Dipole ( $e,e$ ) spectroscopy of ref 119. For the higher ES, we give the contributions given for the two vibrational quanta. <sup>m</sup>Stark measurements of the 0–0 bands from ref 120. Note that the value for the lowest ES is considered as an upper limit in this work. The sign of the dipole is assumed to be consistent with theory. <sup>n</sup>Dipole ( $\gamma,\gamma'$ ) measurements from ref 121, summing over the different vibrational contributions. <sup>o</sup>Two-photon laser induced fluorescence spectroscopy measurement of the Stark effect from ref 122. The sign of the dipole is assumed to be consistent with theory.

comparison, while the basis set effects are far from being negligible for the  $^1\Sigma_u^+$  ES, it is definitely possible to establish robust CBS  $f$  values for this transition.

For the vertical excitation energies, our TBE/CBS of 12.83, 13.27, and 13.57 eV for the three lowest  $^1\Pi_u$  transitions and of 12.96 eV for the lowest  $^1\Sigma_u^+$  transition are all in reasonable agreement with current state-of-the-art. Indeed, as can be seen from the bottom of Table 6, these values are close to the experimental vertical data deduced elsewhere<sup>130</sup> and to our recent FCI/CBS estimates.<sup>5</sup> When turning to the oscillator strengths, there is quite a diversity in the experimentally measured values (see Table 8 of ref 129 for integrated values and Table 1 of ref 133 for individual vibronic contributions from various earlier studies). For the  $^1\Sigma_u^+$  transition, several estimates are available and they show a wide range on both the theoretical and experimental sides (see Table 3 of ref 134), and our TBE/CBS  $f$  value of 0.207 is reasonably in line with the most recent electron impact measurement that we have found (0.223),<sup>131</sup> yet significantly smaller than a value obtained by electron scattering (0.279).<sup>129</sup> For the first and third  $^1\Pi_u$  transitions, our estimates of the oscillator strength come with large error bars ( $0.22 \pm 0.06$  and  $0.10 \pm 0.03$ , respectively), which nevertheless cover the most recent experimental values (0.243 and 0.080),<sup>129</sup> an outcome that we found satisfying. As stated above, no reasonable estimate could be obtained for the oscillator strengths of the remaining transition. It is likely that high-level multireference calculations would be welcome in this specific case.

**3.6. Ethylene.** The ESs of this model  $\pi$ -conjugated hydrocarbon have puzzled chemists for years, in particular, the relative ordering and nature of the two lowest singlet ESs considered here (Table 7). As can be seen, the oscillator strength of the lowest Rydberg state of  $B_{3u}$  symmetry is much too large with 6-31+G(d) but rapidly converges in the Dunning series, the addition of a second set of diffuse functions playing no significant role. In fact, the  $f$  values for this transition converges faster when climbing the methodology ladder than the  $\Delta E_{\text{vert}}$  values. For the valence  $\pi \rightarrow \pi^*$   $B_{1u}$  transition, CCSD seems to slightly overestimate the oscillator strength and the convergence with basis set size is nearly reached with aug-cc-pVTZ. Our best estimates are 7.42 eV ( $f = 0.076$ ) and 7.90 eV ( $f = 0.338$ ) for the Rydberg and valence transitions, respectively.

On the theoretical side, the most advanced theoretical study of ethylene's ESs likely remains the 2014 investigation of Feller *et al.*<sup>88</sup> With their best composite theory, these authors reported transition energies of 7.45 and 8.00 eV with respective  $f$  values of 0.069 and 0.333 (see footnotes of Table 7 for details). One can also compare to the values of ref 5: FCI/CBS estimates of 7.43 and 7.92 eV with CC3/AVTZ  $f$  values of 0.078 and 0.346, respectively. Older studies report oscillator strengths of 0.389 for the valence state at the CCSDT/TZVP level,<sup>39</sup> and 0.078 and 0.358 with CCSD.<sup>139</sup> The experimental measurements of the oscillator strength do not allow us to attribute values to individual transitions because of strong overlapping.<sup>140</sup> The generally used experimental reference values are 0.34 or 0.29 for the valence transition, both estimates being obtained from measurements of the vacuum absorption spectrum performed in 1953<sup>138</sup> and 1955,<sup>141</sup> respectively. However, a more recent dipole ( $e,e$ ) spectroscopy study suggests that the originally measured oscillator strengths in the 7.4–8.0 eV regions are probably too low by *ca.* 10–15%.<sup>140</sup> Our TBE of 0.338 is therefore

Table 6. Vertical Transition Energies  $\Delta E_{\text{vert}}$  and Oscillator Strengths  $f$  Determined for  $\text{N}_2$  (GS Geometry)<sup>a</sup>

| basis         | method           | <sup>1</sup> $\Pi_u$ (Ryd) |   | <sup>1</sup> $\Sigma_u^+$ (Ryd) |  | <sup>1</sup> $\Pi_u$ (Ryd) |   | <sup>1</sup> $\Pi_u$ (Ryd) |                          |
|---------------|------------------|----------------------------|---|---------------------------------|--|----------------------------|---|----------------------------|--------------------------|
|               |                  | $\Delta E_{\text{vert}}$   | $f$                                     | $\Delta E_{\text{vert}}$        | $f$                                    | $\Delta E_{\text{vert}}$   | $f$                                       | $\Delta E_{\text{vert}}$   | $f$                      |
| aug-cc-pVDZ   | CCSD             | 13.451                     | 0.531                                   | 13.250                          | 0.311                                  | 13.765                     | 0.014                                     | 14.497                     | 0.148                    |
|               | CCSDT            | 13.174                     | 0.469                                   | 13.131                          | 0.334                                  | 13.591                     | 0.020                                     | 14.228                     | 0.163                    |
|               | CCSDTQ           | 13.131                     | 0.458                                   | 13.109                          | 0.337                                  | 13.560                     | 0.027                                     | 14.221                     | 0.164                    |
|               | CCSDTQP          | 13.127                     | 0.457                                   | 13.107                          | 0.338                                  | 13.558                     | 0.028                                     | 14.216                     | 0.164                    |
| aug-cc-pVTZ   | CCSD             | 13.422                     | 0.439                                   | 13.264                          | 0.263                                  | 13.674                     | 0.053                                     | 14.307                     | 0.136                    |
|               | CCSDT            | 13.140                     | 0.435                                   | 13.118                          | 0.281                                  | 13.455                     | 0.008                                     | 14.034                     | 0.148                    |
|               | CCSDTQ           | 13.095                     | 0.424                                   | 13.090                          | 0.285                                  | 13.419                     | 0.014                                     | 14.014                     | 0.149                    |
| aug-cc-pVQZ   | CCSD             | 13.354                     | 0.357                                   | 13.242                          | 0.242                                  | 13.638                     | 0.113                                     | 14.216                     | 0.134                    |
|               | CCSDT            | 13.108                     | 0.422                                   | 13.088                          | 0.258                                  | 13.372                     | 0.000                                     | 13.935                     | 0.145                    |
| aug-cc-pVSZ   | CCSD             | 13.235                     | 0.266                                   | 13.195                          | 0.219                                  | 13.621                     | 0.181                                     | 14.100                     | 0.126                    |
|               | CCSDT            | 13.037                     | 0.356                                   | 13.039                          |  | 13.306                     | 0.044                                     | 13.816                     | 0.138                    |
| d-aug-cc-pVDZ | CCSD             | 12.784                     | 0.170                                   | 12.822                          | 0.172                                  | 13.640                     | 0.101                                     | 13.537                     | 0.234                    |
|               | CCSDT            | 12.669                     | 0.198                                   | 12.712                          | 0.183                                  | 13.262                     | 0.256                                     | 13.300                     | 0.014                    |
| d-aug-cc-pVTZ | CCSD             | 12.978                     | 0.178                                   | 13.026                          | 0.181                                  | 13.599                     | 0.314                                     | 13.682                     | 0.007                    |
|               | CCSDT            | 12.827                     | 0.224                                   | 12.885                          | 0.193                                  | 13.257                     | 0.168                                     | 13.396                     | 0.073                    |
| d-aug-cc-pVQZ | CCSD             | 13.039                     | 0.181                                   | 13.090                          | 0.184                                  | 13.601                     | 0.276                                     | 13.730                     | 0.043                    |
|               | CCSDT            | 12.876                     | 0.234                                   | 12.939                          | 0.196                                  | 13.256                     | 0.460                                     | 13.443                     | 0.082                    |
| aug-cc-pVTZ   | TBE <sup>b</sup> | 13.090                     | 0.423                                   | 13.088                          | 0.286                                  | 13.417                     | 0.015                                     | 14.009                     | 0.148                    |
| CBS           | TBE <sup>b</sup> | 12.83 ± 0.08               | 0.22 ± 0.06 <sup>c</sup>                | 12.96 ± 0.01                    | 0.207 ± 0.005                          | 13.27 ± 0.07               | <sup>d</sup>                              | 13.57 ± 0.12               | 0.10 ± 0.03 <sup>c</sup> |
| lit.          | th.              | 12.73 <sup>e</sup>         | 0.458 <sup>e</sup>                      | 12.95 <sup>e</sup>              | 0.296 <sup>e</sup>                     | 13.27 <sup>e</sup>         | 0.000 <sup>e</sup>                        |                            |                          |
|               |                  |                            | 0.091 <sup>f</sup> ; 0.063 <sup>g</sup> |                                 | 0.65 <sup>f</sup> ; 0.221 <sup>g</sup> |                            | 0.32 <sup>f</sup> ;<br>0.091 <sup>g</sup> |                            | 0.083 <sup>g</sup>       |
| exp.          |                  | 12.78 <sup>h</sup>         | 0.243 <sup>i</sup>                      | 12.96 <sup>h</sup>              | 0.279 <sup>i</sup>                     | 13.10 <sup>h</sup>         | 0.145 <sup>i</sup>                        |                            | 0.080 <sup>i</sup>       |
|               |                  | 12.90 <sup>j</sup>         |   | 12.98 <sup>j</sup>              | 0.223 <sup>k</sup>                     | 13.24 <sup>j</sup>         |   | 13.63 <sup>j</sup>         |                          |

<sup>a</sup>See the caption of Table 1 for details. <sup>b</sup>See the corresponding footnotes in Table 1. <sup>c</sup>The extrapolation is very challenging because of the mixing, tentative values. <sup>d</sup>Too unstable to report any reasonable CBS estimate. <sup>e</sup>From ref 5: energies are basis set corrected exFCI/aug-cc-pVQZ values and the oscillator strengths are LR-CC3/aug-cc-pVTZ values. Note that a factor of two linked to the degeneracy was incorrectly omitted in this earlier work for the  $\Pi_u$  transitions. <sup>f</sup>RPA values in length gauge from ref 127. <sup>g</sup>SOPA values from ref 128. <sup>h</sup>Experimental vertical values given in ref 127 deduced from spectroscopic data of ref 116. <sup>i</sup>Integrated intensities from electron scattering of ref 129. <sup>j</sup>Experimental vertical values given in ref 130 deduced from spectroscopic data of ref 116. <sup>k</sup>Integrated electron impact induced emission intensities of ref 131.

Table 7. Vertical Transition Energies  $\Delta E_{\text{vert}}$  and Oscillator Strengths  $f$  of Ethylene (GS Geometry)<sup>a</sup>

| basis         | method           | <sup>1</sup> $B_{3u}$ (Ryd) |                    | <sup>1</sup> $B_{1u}$ (Val) |                    |
|---------------|------------------|-----------------------------|--------------------|-----------------------------|--------------------|
|               |                  | $\Delta E_{\text{vert}}$    | $f$                | $\Delta E_{\text{vert}}$    | $f$                |
| 6-31+G(d)     | CCSD             | 7.814                       | 0.152              | 8.275                       | 0.380              |
|               | CCSDT            | 7.725                       | 0.151              | 8.152                       | 0.365              |
|               | CCSDTQ           | 7.722                       | 0.150              | 8.137                       | 0.364              |
|               | CCSDTQP          | 7.722                       | 0.150              | 8.135                       | 0.364              |
| aug-cc-pVDZ   | CCSD             | 7.323                       | 0.080              | 8.035                       | 0.365              |
|               | CCSDT            | 7.294                       | 0.080              | 7.944                       | 0.352              |
|               | CCSDTQ           | 7.303                       | 0.080              | 7.932                       | 0.351              |
| aug-cc-pVTZ   | CCSD             | 7.417                       | 0.078              | 8.020                       | 0.362              |
|               | CCSDT            | 7.365                       | 0.078              | 7.918                       | 0.346              |
| aug-cc-pVQZ   | CCSD             | 7.451                       | 0.078              | 8.023                       | 0.360              |
| d-aug-cc-pVDZ | CCSD             | 7.301                       | 0.078              | 8.008                       | 0.345              |
|               | CCSDT            | 7.273                       | 0.078              | 7.920                       | 0.336              |
| d-aug-cc-pVTZ | CCSD             | 7.409                       | 0.077              | 8.009                       | 0.353              |
|               | CCSDT            | 7.357                       | 0.077              | 7.908                       | 0.339              |
| d-aug-cc-pVQZ | CCSD             | 7.446                       | 0.077              | 8.017                       | 0.355              |
| aug-cc-pVTZ   | TBE <sup>b</sup> | 7.374                       | 0.078              | 7.905                       | 0.345              |
| CBS           | TBE <sup>c</sup> | 7.42 ± 0.02                 | 0.076 ± 0.001      | 7.90 ± 0.01                 | 0.338 ± 0.005      |
| lit.          | th.              | 7.45 <sup>d</sup>           | 0.069 <sup>d</sup> | 8.00 <sup>d</sup>           | 0.333 <sup>d</sup> |
|               |                  | 7.43 <sup>e</sup>           | 0.078 <sup>e</sup> | 7.92 <sup>e</sup>           | 0.348 <sup>e</sup> |
| exp.          |                  | 7.11 <sup>f</sup>           | ~0.04 <sup>g</sup> | 7.60 <sup>f</sup>           | 0.34 <sup>h</sup>  |

<sup>a</sup>See the caption of Table 1 for details. <sup>b</sup>CCSDT/aug-cc-pVTZ values corrected for Q effects using aug-cc-pVDZ and for P effects using 6-31+G(d). <sup>c</sup>See the Computational Methods section. <sup>d</sup>From ref 88: best composite theory for energies, icCAS(12/15)-CI/VDZ + for the oscillator strengths of the Rydberg transition and icINO(12/16)-CI/VDZ + extrapolated to FCI for the oscillator strengths of the valence transition. <sup>e</sup>FCI/CBS (for transition energies) and CC3/aug-cc-pVTZ (for  $f$ ) values from ref 5. <sup>f</sup>Experimental values collected in ref 135 (see the discussions in refs 2,88,136). <sup>g</sup>From ref 137 (see text). <sup>h</sup>Vacuum absorption from ref 138.

reasonably in line with the current experimental knowledge. For the Rydberg ES, the only experimental estimate we are aware of has been reported in 1969 as a “total  $f$  perhaps about 0.04”.<sup>137</sup> Given the consistency of all theoretical estimates, it seems rather reasonable to state that our current TBE of 0.076 is significantly more trustworthy. In ethylene, in contrast to  $N_2$ , theory has clearly the edge because the considered transitions have different spatial symmetries.

**3.7. Formaldehyde and Thioformaldehyde.** The ESs of formaldehyde have been extensively studied before with almost all possible theoretical approaches,<sup>2,5,45,74,142–155</sup> and we have considered here, two valence and three Rydberg states. Our results are collected in Table 8 for these five ESs. The hallmark  $n \rightarrow \pi^*$  transition behaves nicely from a theoretical point of view, and the convergences of both  $\Delta E_{\text{vert}}$  and  $\mu^{\text{ES}}$  with respect to the basis set size are very quick, with a negligible effect of the second set of diffuse functions. Likewise, the corrections brought by the Q and P terms in the CC expansion are rather negligible, and CCSDT/aug-cc-pVTZ values are trustworthy. The higher-lying  $\pi \rightarrow \pi^*$  valence ES is significantly more challenging as, on the one hand, the second set of diffuse functions significantly increases the transition energy (by *ca.* +0.2 eV), decreases the oscillator strength (by roughly 10%), and greatly amplifies the ES dipole (by a factor of 2 or 3), whereas, on the other hand, going from CCSDT to CCSDTQ yields a non-negligible drop of the computed dipole. Extrapolation to the CBS limit is therefore uneasy for the latter property. The oscillator strengths of the three Rydberg ESs are all relatively small, but their absolute and relative amplitudes are fairly independent on the selected level of theory and basis sets, though double augmentation induces a small decrease of the magnitude of the oscillator strength. The value of  $\mu^{\text{ES}}$  for the lowest-lying Rydberg ES cannot be adequately described with the selected Pople basis set but are easy to extrapolate using Dunning’s series. For the second (third) Rydberg ES, all tested approaches agree on the rather small (moderate) amplitude for  $\mu^{\text{ES}}$ , but the basis set effects are large. For instance, considering the higher-lying Rydberg ES, the CCSDT  $\mu^{\text{ES}}$  value is  $-0.06$  D with 6-31+G(d),  $-2.19$  D with aug-cc-pVDZ, and  $-0.37$  D with d-aug-cc-pVTZ. Clearly it is challenging to obtain a definitive CBS estimate.

A very accurate measurement of  $\mu^{\text{GS}}$  for formaldehyde is available at  $2.3321 \pm 0.0005$  D (molecular beam electric resonance spectroscopy),<sup>159</sup> and our theoretical TBE of  $2.41 \pm 0.01$  D seems slightly too large but is in very good agreement with previous CCSD(T)/CBS ( $2.393$  D)<sup>47</sup> and CCSD(T)/aug-cc-pVQZ ( $2.382$  D) estimates.<sup>166</sup> As early as 2004, Hirata proposed a CCSDT/aug-cc-pVDZ value of  $\mu^{\text{GS}}$  at  $2.33$  D,<sup>74</sup> right on the experimental spot, but an experimental geometry was used and the orbital relaxation effects were neglected, which might have induced a very slight error compensation. For the hallmark lowest  $n \rightarrow \pi^*$  transition, one can find several experimental estimates of  $\mu^{\text{ES}}$ :  $1.48 \pm 0.07$ ,<sup>172</sup>  $1.56 \pm 0.07$ ,<sup>173</sup>  $1.4 \pm 0.1$ ,<sup>174</sup>  $1.53 \pm 0.11$ ,<sup>160</sup> and  $1.47$  D.<sup>164</sup> Somehow surprisingly, the most recent value obtained by Stark quantum beat spectroscopy has hardly been considered as reference in earlier theoretical studies than the maximal measured value of  $1.56$  D. On the theory side, one can highlight two significant earlier contributions (on the ES geometry):  $1.48$  D (CCSDT/aug-cc-pVDZ)<sup>74</sup> and  $1.73$  D (CC2/aug-cc-pVQZ).<sup>45</sup> We somehow reconcile these earlier results by using both large basis sets and high CC levels, and considering both geometries, leading to a TBE/CBS of  $1.52 \pm 0.01$  D for the adiabatic value,

right at the center of the experimental cloud. It is noteworthy that the geometrical relaxation induces a non-negligible increase in the magnitude of the dipole moment for the  $A_2$  ( $1A''$ ) ES. We indeed found a TBE/CBS value of  $1.36 \pm 0.02$  D for the GS geometry. For this  $\mu_{\text{vert}}^{\text{ES}}$  earlier estimates include the  $1.46$  D (CASPT2/TZVP)<sup>2</sup> and  $1.38$  D (CC2/aug-cc-pVTZ).<sup>43</sup> For the lowest  $B_2$  Rydberg transition, we are aware of one experiment only (polarized electrochromism), leading to an ES dipole of  $-0.33 \pm 0.16$  D.<sup>162,163</sup> Although theory does confirm the sign change as compared to the GS, it returns a much larger amplitude for the dipole with  $-2.15 \pm 0.03$  D (GS structure) or  $-1.66 \pm 0.03$  D (ES geometry). At the CCSDT/aug-cc-pVDZ level, Hirata reported  $-2.52$  D (vertical),<sup>74</sup> likely the best previous estimate. This significant discrepancy between theory and experiment was previously attributed to a (experimental) mixing between the two lowest-lying  $B_2$  transitions.<sup>157</sup> It seems reasonable to state that theory has the edge in this case. For the higher-lying ES, no Stark effect measurement is available, and our values are very likely more accurate than the previous ones reported at the CCSDT level but with a rather small basis set.<sup>74</sup> Nevertheless, the CBS extrapolation is uneasy, and large error bars are obtained for all these high-lying ESs. The oscillator strengths of the three lowest Rydberg transitions,  $B_2(n \rightarrow 3s)$ ,  $B_2(n \rightarrow 3p)$ , and  $A_1(n \rightarrow 3s)$ , have been respectively measured as  $0.038$ ,  $0.017 \pm 0.02$ , and  $0.038 \pm 0.04$  (absorption spectroscopy),<sup>175</sup>  $0.028$ ,  $0.017$ , and  $0.032$  (EELS),<sup>161</sup>  $0.032$ ,  $0.019$ , and  $0.036$  (absorption),<sup>176</sup> and  $0.041$ ,  $0.028$ , and  $0.061$  [dipole ( $e, e$ ) spectroscopy].<sup>165</sup> Although the orders of magnitude are consistent with the present calculations, the theoretical values do not follow the same ranking as they yield  $f$  values of  $0.020$ ,  $0.035$ , and  $0.050$ . Such a discrepancy has been attributed by other groups to the difficulty of assigning individual vibronic bands to a specific electronic transition in the experimental spectra.<sup>74,177</sup> Interestingly, our current values agree very well with previous theoretical estimates, which returned  $0.018$ ,  $0.040$ , and  $0.043$  (MR-AQCC-LRT),<sup>156</sup>  $0.025$ ,  $0.041$ , and  $0.058$  (CCSDT),<sup>74</sup>  $0.018$ ,  $0.035$ , and  $0.050$  (EOM-CCSD),<sup>158</sup> and  $0.021$ ,  $0.037$ , and  $0.052$  (CC3).<sup>5</sup> For the brighter  $\pi \rightarrow \pi^*$  transition, we are not aware of experimental  $f$  data, but theoretical values reported in previous studies are of the order of  $0.1$ :  $0.100$ ,<sup>156</sup>  $0.093$ ,<sup>158</sup> and  $0.135$ ,<sup>5</sup> and our current TBE of  $0.107 \pm 0.002$  lies in the middle of these earlier estimates. In the original Thiel benchmark, the next  $A_1$  ES with a larger  $f$  was actually considered.<sup>2</sup>

In thioformaldehyde (Table 9), one notes relatively stable  $\Delta E_{\text{vert}}$  and  $\mu^{\text{ES}}$  for the lowest dipole-forbidden  $A_2$  transition: the convergence is rather fast with respect to both CC expansion and basis set size, so we can safely report accurate TBE/CBS for both the GS and ES structures. The change in the ES dipole between the two geometries is limited as well, contrasting with formaldehyde. This is because there is no puckering effect in thioformaldehyde’s  $A_2$  ES: the true minimum belongs to the  $C_{2v}$  point group.<sup>33,178,179</sup> For the first Rydberg transition ( $B_2$ ) the impact of the basis set size is logically more pronounced with, for example, a  $+0.76$  D change between the CCSDT/aug-cc-pVTZ and CCSDT/d-aug-cc-pVTZ dipoles, making the TBE/CBS extrapolation uncertainty larger than for the  $A_2$  ES. The difference between the values of  $\mu^{\text{ES}}$  determined at the GS and ES equilibrium geometries is also larger for the Rydberg excitation than for the lowest transition, despite the planarity of all geometries. When selecting Dunning’s basis sets, the weak oscillator strength of

Table 8. GS Dipole Moment  $\mu^{GS}$ , Vertical Transition Energies  $\Delta E_{\text{vert}}$ , Oscillator Strengths  $f$ , and ES Dipole Moments,  $\mu_{\text{vert}}^{\text{ES}}$  and  $\mu_{\text{adia}}^{\text{ES}}$ , Determined for Formaldehyde<sup>a</sup>

| basis         | method           | $^1A_1$            |                          | $^1A_2(\text{Val}, n \rightarrow \pi^*)$ |                                 | $^1B_2(\text{Ryd}, n \rightarrow 3s)$ |   |                    |                           |
|---------------|------------------|--------------------|--------------------------|--|---------------------------------|---------------------------------------|---|--------------------|---------------------------|
|               |                  | $\mu^{GS}$         | $\Delta E_{\text{vert}}$ | $\mu_{\text{vert}}^{\text{ES}}$          | $\mu_{\text{adia}}^{\text{ES}}$ | $\Delta E_{\text{vert}}$              | $f$                                     |                    |                           |
| 6-31+G(d)     | CCSD             | 2.584              | 4.031                    | 1.710                                    | 1.870                           | 7.238                                 | 0.017                                   | -0.901             | -0.479                    |
|               | CCSDT            | 2.529              | 4.012                    | 1.649                                    | 1.790                           | 7.232                                 | 0.021                                   | -1.459             | -0.990                    |
|               | CCSDTQ           | 2.518              | 4.022                    | 1.629                                    | 1.751                           | 7.279                                 | 0.020                                   | -1.364             | -0.906                    |
|               | CCSDTQP          | 2.517              | 4.023                    | 1.627                                    | 1.746                           | 7.287                                 | 0.020                                   | -1.342             | -0.885                    |
|               | CCSD             | 2.427              | 4.020                    | 1.397                                    | 1.602                           | 7.043                                 | 0.018                                   | -2.078             | -1.634                    |
|               | CCSDT            | 2.368              | 3.986                    | 1.337                                    | 1.524                           | 7.040                                 | 0.020                                   | -2.457             | -1.976                    |
|               | CCSDTQ           | 2.356              | 3.997                    | 1.319                                    | 1.486                           | 7.091                                 | 0.020                                   | -2.403             | -1.932                    |
|               | CCSD             | 2.457              | 4.013                    | 1.416                                    | 1.620                           | 7.231                                 | 0.018                                   | -1.929             | -1.476                    |
|               | CCSDT            | 2.389              | 3.954                    | 1.346                                    | 1.534                           | 7.165                                 | 0.020                                   | -2.379             | -1.873                    |
|               | CCSD             | 2.475              | 4.024                    | 1.436                                    | 1.635                           | 7.296                                 | 0.018                                   | -1.861             | -1.406                    |
| d-aug-cc-pVDZ | CCSD             | 2.417              | 4.012                    | 1.386                                    | 1.596                           | 7.027                                 | 0.016                                   | -1.839             | -1.410                    |
|               | CCSDT            | 2.359              | 3.978                    | 1.327                                    | 1.518                           | 7.024                                 | 0.019                                   | -2.282             | -1.803                    |
|               | CCSD             | 2.454              | 4.011                    | 1.418                                    | 1.619                           | 7.224                                 | 0.017                                   | -1.751             | -1.309                    |
|               | CCSDT            | 2.387              | 3.952                    | 1.347                                    | 1.533                           | 7.158                                 | 0.020                                   | -2.248             | -1.743                    |
| d-aug-cc-pVQZ | CCSD             | 2.475              | 4.023                    | 1.439                                    | 1.636                           | 7.192                                 | 0.018                                   | -1.747             | -1.299                    |
|               | TBE <sup>b</sup> | 2.375              | 3.966                    | 1.325                                    | 1.491                           | 7.225                                 | 0.020                                   | -2.302             | -1.809                    |
| aug-cc-pVTZ   | TBE <sup>b</sup> | 2.41 ± 0.01        | 3.99 ± 0.01              | 1.36 ± 0.01                              | 1.52 ± 0.01                     | 7.34 ± 0.01                           | 0.020 ± 0.001                           | -2.15 ± 0.03       | -1.66 ± 0.03              |
|               | th.              | 2.393 <sup>c</sup> | 3.98 <sup>d</sup>        | 1.33 <sup>c</sup>                        | 1.48 <sup>e</sup>               | 7.12 <sup>d</sup>                     | 0.018 <sup>f</sup> , 0.025 <sup>e</sup> | -2.52 <sup>e</sup> | -3.45 <sup>f</sup>        |
| CBS           | lit.             | 2.33 <sup>c</sup>  | 3.97 <sup>g</sup>        |  | 1.73 <sup>h</sup>               | 7.30 <sup>g</sup>                     |   |                    |                           |
|               |                  | 2.44 <sup>i</sup>  | 3.98 <sup>j</sup>        | 1.46 <sup>j</sup>                        |                                 |                                       |   |                    |                           |
|               | exp.             | 2.332 <sup>k</sup> | 4.07 <sup>l</sup>        |  | 1.53 ± 0.11 <sup>m</sup>        | 7.11 <sup>k</sup>                     | 0.028 <sup>n</sup>                      |                    | -0.33 ± 0.16 <sup>o</sup> |
|               |                  |                    |                          | 1.47 <sup>p</sup>                        |                                 | 0.041 <sup>q</sup>                    |   |                    |                           |

| basis         | method           | $^1B_2(\text{Ryd}, n \rightarrow 3p)$ |               | $^1A_1(\text{Val}, \pi \rightarrow \pi^*)$ |               |
|---------------|------------------|---------------------------------------|---------------|--|---------------|
|               |                  | $\Delta E_{\text{vert}}$              | $f$           | $\Delta E_{\text{vert}}$                   | $f$           |
| 6-31+G(d)     | CCSD             | 7.994                                 | 0.042         | 8.282                                      | 0.060         |
|               | CCSDT            | 8.007                                 | 0.040         | 8.295                                      | 0.058         |
|               | CCSDTQ           | 8.045                                 | 0.040         | 8.341                                      | 0.058         |
|               | CCSDTQP          | 8.051                                 | 0.041         | 8.350                                      | 0.058         |
|               | CCSD             | 7.993                                 | 0.044         | 8.052                                      | 0.058         |
| aug-cc-pVDZ   | CCSD             | 8.002                                 | 0.042         | 8.068                                      | 0.057         |
|               | CCSDTQ           | 8.045                                 | 0.042         | 8.119                                      | 0.057         |
|               | CCSD             | 8.120                                 | 0.040         | 8.210                                      | 0.054         |
|               | CCSDT            | 8.070                                 | 0.038         | 8.164                                      | 0.052         |
|               | CCSD             | 8.153                                 | 0.039         | 8.267                                      | 0.053         |
| aug-cc-pVTZ   | CCSD             | 7.834                                 | 0.036         | 7.962                                      | 0.049         |
|               | CCSDT            | 7.846                                 | 0.035         | 7.983                                      | 0.049         |
|               | CCSD             | 8.026                                 | 0.035         | 8.169                                      | 0.050         |
|               | CCSDT            | 7.978                                 | 0.033         | 8.126                                      | 0.049         |
|               | CCSD             | 8.095                                 | 0.035         | 8.240                                      | 0.050         |
| d-aug-cc-pVQZ | TBE <sup>b</sup> | 8.119                                 | 0.039         | 8.224                                      | 0.052         |
|               | CBS              | 8.16 ± 0.02                           | 0.035 ± 0.002 | 8.28 ± 0.04                                | 0.050 ± 0.001 |
| aug-cc-pVTZ   | TBE <sup>b</sup> |                                       |               |  |               |
|               | CBS              |                                       |               |  |               |

Table 8. continued

| basis | method | $^1B_2$ (Ryd, $n \rightarrow 3p$ ) |   |                                 | $^1A_1$ (Ryd, $n \rightarrow 3p$ ) |   |                                 | $^1A_1$ (Val, $\pi \rightarrow \pi^*$ ) |   |                                 |
|-------|--------|------------------------------------|---|---------------------------------|------------------------------------|---|---------------------------------|---|---|---------------------------------|
|       |        | $\Delta E_{\text{vert}}$           | $f$                                     | $\mu_{\text{vert}}^{\text{ES}}$ | $\Delta E_{\text{vert}}$           | $f$                                     | $\mu_{\text{vert}}^{\text{ES}}$ | $\Delta E_{\text{vert}}$                | $f$                                     | $\mu_{\text{vert}}^{\text{ES}}$ |
| lit.  | th.    | 7.94 <sup>d</sup>                  | 0.040 <sup>d</sup> ; 0.041 <sup>e</sup> | 0.85 <sup>e</sup>               | 8.16 <sup>d</sup>                  | 0.043 <sup>d</sup> ; 0.058 <sup>e</sup> | -2.16 <sup>e</sup>              | 9.83 <sup>d</sup>                       | 0.100 <sup>d</sup>                      |                                 |
|       | exp.   | 8.14 <sup>g</sup>                  | 0.037 <sup>g</sup> ; 0.035 <sup>f</sup> |                                 | 8.27 <sup>g</sup>                  | 0.052 <sup>g</sup> ; 0.050 <sup>f</sup> |                                 | 9.26 <sup>g</sup>                       | 0.135 <sup>g</sup> ; 0.093 <sup>f</sup> |                                 |
|       |        | 7.97 <sup>f</sup>                  | 0.017 <sup>h</sup>                      |                                 | 8.14 <sup>f</sup>                  | 0.032 <sup>h</sup>                      |                                 |   |   |                                 |
|       |        |                                    | 0.018 <sup>g</sup>                      |                                 |                                    | 0.061 <sup>g</sup>                      |                                 |   |   |                                 |

<sup>a</sup>See the caption of Table 1 for details. <sup>b</sup>See the corresponding footnotes in Table 7. <sup>c</sup>CCSD(T)/CBS value from ref 47. <sup>d</sup>MR-AQC-LRT calculations from ref 156. <sup>e</sup>CCSDT/aug-cc-pVDZ results from ref 74. <sup>f</sup>MRDCI value from ref 157. <sup>g</sup>exFCI/aug-cc-pVTZ transition energies corrected for basis set effects up to d-aug-cc-pVTZ and LR-CC3/aug-cc-pVTZ for  $f$  from ref 5. <sup>h</sup>CC2/aug-cc-pVQZ figure from ref 45. <sup>i</sup>EOM-CCSD from ref 158. <sup>j</sup>CASPT2/TZVP values from ref 2. <sup>k</sup>Electric resonance spectroscopy from ref 159. <sup>l</sup>Various experimental sources collected in ref 135. <sup>m</sup>Stark effect measurement on lineshapes from ref 160. <sup>n</sup>EELS values from ref 161. <sup>o</sup>Values measured from polarized electrochromism reported in refs 162 and 163. <sup>p</sup>Stark effect from quantum beat spectroscopy from ref 164. <sup>q</sup>Dipole ( $e$ ) spectroscopy from ref 165.

the  $B_2$  transition always falls in a rather tight window (0.011–0.015). The valence  $A_1(\pi \rightarrow \pi^*)$  transition is clearly no cakewalk: not only does the enlargement of the basis set yields significant changes of  $\mu^{\text{ES}}$  (e.g., +0.49 D from CCSDT/aug-cc-pVTZ to CCSDT/d-aug-cc-pVTZ), but, in addition, the impact of the quadruples in the CC expansion becomes significant: the Q term induces a drop of  $\mu^{\text{ES}}$  by ca. -0.40 D and a decrease in  $f$  by ca. 15%. For this transition, CCSD is clearly insufficient to obtain accurate ES properties. A chemical understanding of the underlying reasons for this large Q effect in the  $A_1$  ES of thioformaldehyde would likely require an in-depth analysis of the various densities determined at various levels of theory, which is beyond our scope.

The value of  $\mu^{\text{GS}}$  in thioformaldehyde was measured very accurately:  $1.6491 \pm 0.0004$  D<sup>159</sup> and our TBE of  $1.73 \pm 0.01$  D is slightly higher. The same comment applies to a previous CCSD(T)/aug-cc-pVQZ value of (1.700 D)<sup>166</sup> and a CC2/aug-cc-pVQZ value of 1.72 D.<sup>45</sup> Like in formaldehyde, one can find a series of Stark measurements relying on various spectroscopic techniques for the lowest  $^1A_2$  ES. Quite a range of magnitudes have been reported for  $\mu^{\text{ES}}$ :  $0.79 \pm 0.04$  D (absorption spectroscopy),<sup>180</sup>  $0.838 \pm 0.008$  D (laser-induced fluorescence excitation),<sup>181</sup>  $0.850 \pm 0.002$  D (microwave-optical double resonance),<sup>168</sup> and  $0.815 \pm 0.020$  D (intermodulated fluorescence).<sup>171</sup> Obviously, the error bars of these measurements are not overlapping, but the latter work warns that values between 0.77 and 0.93 D can be obtained.<sup>171</sup> Our TBEs of  $0.88 \pm 0.01$  D (GS geometry) and  $0.89 \pm 0.01$  D (ES geometry) are therefore obviously compatible with the experimental measures. The only previous wave function-based TBE we are aware of is the CC2/aug-cc-pVQZ value of 0.96 D estimated by Hellweg (ES geometry)<sup>45</sup> that appears approximately 0.10 D too large. For the second ES (of Rydberg nature), we found only one measurement of the Stark effect (on the absorption spectrum) that led to a  $\mu^{\text{ES}}$  value of  $-2.2 \pm 0.3$  D.<sup>169</sup> Theory clearly confirms the flip of the dipole as compared to the GS, but our TBEs are significantly larger than this experimental value, irrespective of the considered geometry:  $-3.27$  (GS geometry) and  $-3.05$  D (ES geometry). Given the significant basis set dependence of  $\mu^{\text{ES}}$  of this state, one clearly needs to be cautious but it is nevertheless likely that the experimental value of  $-2.2$  D is too low. To the best of our knowledge, there is no previous published value of  $\mu^{\text{ES}}$  for the  $A_1$  ES. Concerning the oscillator strengths, the previous TBEs are likely our CC3/aug-cc-pVTZ values: 0.012 ( $B_1$ ) and 0.178 ( $A_1$ ),<sup>5</sup> which are consistent with the new values listed in Table 9. On the “experimental side”, an estimate of 0.38 was proposed for the valence transition,<sup>182</sup> but it is based on an empirical ratio of 10 compared to an earlier estimate of the oscillator strength for the corresponding Rydberg ES of formaldehyde.<sup>175</sup> We trust that our current TBEs are significantly more accurate.

**3.8. Nitroxyl and Fluorocarbene.** Table 10 provides the dipole moments and transition energies of the lowest ES of HNO. Although this transition is not strictly forbidden by symmetry, all methods return very low  $f$  values ( $<0.001$ ). Thus, we have not bothered reporting the values of the oscillator strength.

As can be seen in Table 10, the convergences with respect to the CC excitation order and basis size are rather fast: quadruples tune the dipole par  $\sim -0.01$  D only, and basis set extension beyond triple- $\zeta$  is unnecessary. In other words, CCSDT/aug-cc-pVTZ provides very accurate estimates and

Table 9. GS Dipole Moment  $\mu^{\text{GS}}$ , Vertical Transition Energies  $\Delta E_{\text{vert}}^{\text{ES}}$ , Oscillator Strengths  $f$ , and ES Dipole Moments,  $\mu_{\text{vert}}^{\text{ES}}$  and  $\mu_{\text{adia}}^{\text{ES}}$ , Determined for Thioformaldehyde<sup>a</sup>

| basis         | method           | <sup>1</sup> A <sub>1</sub> ( <sup>1</sup> Val, n → $\pi^*$ ) |                                      |                                 | <sup>1</sup> B <sub>2</sub> (Ryd, n → 4s) |                                      |                    | <sup>1</sup> A <sub>1</sub> (Val, $\pi$ → $\pi^*$ ) |                                 |                                      |                    |                                 |
|---------------|------------------|---|--------------------------------------|---------------------------------|---|--------------------------------------|--------------------|---|---------------------------------|--------------------------------------|--------------------|---------------------------------|
|               |                  | $\mu^{\text{GS}}$   | $\Delta E_{\text{vert}}^{\text{ES}}$ | $\mu_{\text{vert}}^{\text{ES}}$ | $\mu_{\text{adia}}^{\text{ES}}$           | $\Delta E_{\text{vert}}^{\text{ES}}$ | $f$                | $\mu_{\text{vert}}^{\text{ES}}$                     | $\mu_{\text{adia}}^{\text{ES}}$ | $\Delta E_{\text{vert}}^{\text{ES}}$ | $f$                | $\mu_{\text{vert}}^{\text{ES}}$ |
| 6-31+G(d)     | CCSD             | 1.747   | 2.302                                | 0.933                           | 0.968                                     | 5.937                                | 0.019              | -3.378  | -3.070                          | 6.961                                | 0.261              | 1.964                           |
|               | CCSDT            | 1.733   | 2.244                                | 0.948                           | 0.990                                     | 5.875                                | 0.018              | -3.570  | -3.257                          | 6.790                                | 0.223              | 1.745                           |
|               | CCSDTQ           | 1.720   | 2.246                                | 0.919                           | 0.947                                     | 5.890                                | 0.019              | -3.563  | -3.253                          | 6.713                                | 0.191              | 1.334                           |
|               | CCSDTQP          | 1.719   | 2.247                                | 0.917                           | 0.943                                     | 5.893                                | 0.019              | -3.562  | -3.252                          | 6.708                                | 0.189              | 1.305                           |
| aug-cc-pVDZ   | CCSD             | 1.742   | 2.325                                | 0.851                           | 0.873                                     | 5.841                                | 0.012              | -3.938  | -3.693                          | 6.749                                | 0.251              | 1.875                           |
|               | CCSDT            | 1.716   | 2.253                                | 0.870                           | 0.898                                     | 5.796                                | 0.011              | -4.140  | -3.885                          | 6.597                                | 0.182              | 1.753                           |
|               | CCSDTQ           | 1.704   | 2.255                                | 0.848                           | 0.864                                     | 5.817                                | 0.011              | -4.134  | -3.885                          | 6.512                                | 0.152              | 1.264                           |
|               | CCSD             | 1.737   | 2.291                                | 0.848                           | 0.870                                     | 5.970                                | 0.014              | -3.374  | -3.149                          | 6.633                                | 0.206              | 2.379                           |
| aug-cc-pVTZ   | CCSD             | 1.706   | 2.207                                | 0.865                           | 0.890                                     | 5.900                                | 0.012              | -3.665  | -3.422                          | 6.467                                | 0.163              | 1.698                           |
|               | CCSDT            | 1.759   | 2.296                                | 0.869                           | 0.890                                     | 6.018                                | 0.014              | -3.162  | -2.944                          | 6.607                                | 0.200              | 2.385                           |
|               | CCSD             | 1.735   | 2.324                                | 0.858                           | 0.877                                     | 5.804                                | 0.015              | -3.258  | -3.055                          | 6.678                                | 0.165              | -0.038                          |
|               | CCSDT            | 1.709   | 2.252                                | 0.875                           | 0.901                                     | 5.761                                | 0.014              | -3.495  | -3.281                          | 6.577                                | 0.191              | 1.749                           |
| d-aug-cc-pVTZ | CCSD             | 1.737   | 2.291                                | 0.851                           | 0.872                                     | 5.958                                | 0.015              | -3.050  | -2.847                          | 6.627                                | 0.206              | 2.376                           |
|               | CCSDT            | 1.707   | 2.207                                | 0.867                           | 0.892                                     | 5.888                                | 0.013              | -3.379  | -3.154                          | 6.463                                | 0.162              | 2.193                           |
|               | CCSD             | 1.759   | 2.296                                | 0.871                           | 0.892                                     | 6.012                                | 0.014              | -2.999  | -2.794                          | 6.604                                | 0.199              | 2.383                           |
|               | TBE <sup>b</sup> | 1.694   | 2.210                                | 0.840                           | 0.851                                     | 5.923                                | 0.013              | -3.658  | -3.421                          | 6.377                                | 0.135              | 1.179                           |
| CBS           | TBE <sup>b</sup> | 1.73 ± 0.01   | 2.22 ± 0.01                          | 0.088 ± 0.01                    | 0.089 ± 0.01                              | 6.01 ± 0.01                          | 0.013 ± 0.001      | -3.27 ± 0.03  | -3.05 ± 0.02                    | 6.33 ± 0.01                          | 0.13 ± 0.01        | 1.20 ± 0.01                     |
|               | th.              | 1.700 <sup>c</sup>  | 2.20 <sup>d</sup>                    | 0.96 <sup>e</sup>               | 0.96 <sup>e</sup>                         | 5.99 <sup>d</sup>                    | 0.012 <sup>f</sup> |   |                                 | 6.34 <sup>g</sup>                    | 0.178 <sup>f</sup> |                                 |
| lit.          | exp.             | 1.649 <sup>h</sup>  | 2.033 <sup>i</sup>                   | 0.850 ± 0.002 <sup>j</sup>      | 0.850 ± 0.002 <sup>j</sup>                | 5.841 <sup>i</sup>                   |                    |   |                                 | 6.60 <sup>i</sup>                    |                    |                                 |
|               |                  | 1.647 <sup>i</sup>  |                                      | 0.815 ± 0.020 <sup>m</sup>      | 0.815 ± 0.020 <sup>m</sup>                |                                      |                    |   |                                 |                                      |                    |                                 |

<sup>a</sup>See the caption of Table 1 for details. <sup>b</sup>See the corresponding footnotes in Table 7. <sup>c</sup>CCSD(T)/aug-cc-pVQZ from ref 166. <sup>d</sup>exFCI/aug-cc-pVTZ transition energies corrected for basis set effects up to d-aug-cc-pVQZ from ref 5. <sup>e</sup>CC2/aug-cc-pVQZ from ref 45. <sup>f</sup>LR-CC3/aug-cc-pVTZ  $f$  from ref 5. <sup>g</sup>CCSDTQ/aug-cc-pVDZ transition energy corrected for basis set effects up to d-aug-cc-pVQZ from ref 5. <sup>h</sup>Molecular beam electric resonance value from ref 159. <sup>i</sup>0–0 energies listed in Table 13 of ref 167. <sup>j</sup>Microwave-optical double resonance measurements of Stark effect from ref 168. <sup>k</sup>Stark effect on the absorption spectrum from ref 169. <sup>l</sup>Stark effect measurement on the microwave spectra from ref 170. <sup>m</sup>Intermodulated fluorescence of the Stark effect from ref 171.

**Table 10.** GS Dipole Moment  $\mu^{\text{GS}}$ , Vertical Transition Energies  $\Delta E_{\text{vert}}$  and ES Dipole Moments,  $\mu_{\text{vert}}^{\text{ES}}$  and  $\mu_{\text{adia}}^{\text{ES}}$  Determined for Nitroxy<sup>a</sup>

| basis         | method           | <sup>1</sup> A'          | <sup>1</sup> A'' (Val, n → π*) |                                 |                                 |
|---------------|------------------|--------------------------|--------------------------------|---------------------------------|---------------------------------|
|               |                  | $\mu^{\text{GS}}$        | $\Delta E_{\text{vert}}$       | $\mu_{\text{vert}}^{\text{ES}}$ | $\mu_{\text{adia}}^{\text{ES}}$ |
| 6-31+G(d)     | CCSD             | 1.902                    | 1.802                          | 1.982                           | 2.111                           |
|               | CCSDT            | 1.876                    | 1.797                          | 1.948                           | 2.076                           |
|               | CCSDTQ           | 1.869                    | 1.799                          | 1.938                           | 2.063                           |
|               | CCSDTQP          | 1.868                    | 1.800                          | 1.927                           | 2.062                           |
| aug-cc-pVDZ   | CCSD             | 1.701                    | 1.779                          | 1.719                           | 1.840                           |
|               | CCSDT            | 1.667                    | 1.767                          | 1.681                           | 1.799                           |
|               | CCSDTQ           | 1.658                    | 1.770                          | 1.670                           | 1.785                           |
| aug-cc-pVTZ   | CCSD             | 1.722                    | 1.756                          | 1.727                           | 1.850                           |
|               | CCSDT            | 1.683                    | 1.737                          | 1.688                           | 1.807                           |
| aug-cc-pVQZ   | CCSD             | 1.735                    | 1.753                          | 1.735                           | 1.859                           |
| d-aug-cc-pVDZ | CCSD             | 1.695                    | 1.778                          | 1.709                           | 1.831                           |
|               | CCSDT            | 1.661                    | 1.766                          | 1.671                           | 1.790                           |
| d-aug-cc-pVTZ | CCSD             | 1.720                    | 1.755                          | 1.724                           | 1.847                           |
|               | CCSDT            | 1.681                    | 1.737                          | 1.685                           | 1.804                           |
| d-aug-cc-pVQZ | CCSD             | 1.735                    | 1.753                          | 1.679                           | 1.795                           |
| aug-cc-pVTZ   | TBE <sup>b</sup> | 1.674                    | 1.740                          | 1.676                           | 1.791                           |
| CBS           | TBE <sup>b</sup> | 1.69 ± 0.01              | 1.73 ± 0.01                    | 1.69 ± 0.01                     | 1.80 ± 0.01                     |
| lit.          | th.              | 1.654 <sup>c</sup>       | 1.74 <sup>d</sup>              |                                 |                                 |
|               | exp.             | 1.67 ± 0.03 <sup>e</sup> | 1.63 <sup>f</sup>              |                                 | 1.69 ± 0.01 <sup>g</sup>        |
|               |                  | 1.62 ± 0.02 <sup>h</sup> |                                |                                 |                                 |

<sup>a</sup>We report the norm of the dipoles. See the caption of Table 1 for details. <sup>b</sup>See the corresponding footnotes in Table 7. <sup>c</sup>CCSD(T)/CBS value from ref 47. <sup>d</sup>Unpublished exFCI/aug-cc-pVTZ value (from our groups). <sup>e</sup>From microwave spectroscopy (ref 183). <sup>f</sup>0-0 energy from ref 184 and references therein. <sup>g</sup>Microwave optical double resonance value from ref 185. <sup>h</sup>From Stark effect measurements (ref 186).

**Table 11.** GS Dipole Moment  $\mu^{\text{GS}}$ , Vertical Transition Energies  $\Delta E_{\text{vert}}$ , Oscillator Strengths  $f$ , and ES Dipole Moments,  $\mu_{\text{vert}}^{\text{ES}}$  and  $\mu_{\text{adia}}^{\text{ES}}$  Determined for Fluorocarbene<sup>a</sup>

| basis         | method           | <sup>1</sup> A'    | <sup>1</sup> A''         |                    |                                 |
|---------------|------------------|--------------------|--------------------------|--------------------|---------------------------------|
|               |                  | $\mu^{\text{GS}}$  | $\Delta E_{\text{vert}}$ | $f$                | $\mu_{\text{vert}}^{\text{ES}}$ |
| 6-31+G(d)     | CCSD             | 1.572              | 2.581                    | 0.009              | 1.316                           |
|               | CCSDT            | 1.552              | 2.573                    | 0.009              | 1.287                           |
|               | CCSDTQ           | 1.549              | 2.577                    | 0.009              | 1.282                           |
|               | CCSDTQP          | 1.549              | 2.578                    | 0.009              | 1.282                           |
| aug-cc-pVDZ   | CCSD             | 1.451              | 2.541                    | 0.007              | 0.991                           |
|               | CCSDT            | 1.430              | 2.529                    | 0.006              | 0.970                           |
|               | CCSDTQ           | 1.428              | 2.534                    | 0.006              | 0.965                           |
| aug-cc-pVTZ   | CCSD             | 1.465              | 2.507                    | 0.006              | 0.991                           |
|               | CCSDT            | 1.441              | 2.493                    | 0.006              | 0.969                           |
| aug-cc-pVQZ   | CCSD             | 1.468              | 2.500                    | 0.006              | 0.994                           |
| d-aug-cc-pVDZ | CCSD             | 1.445              | 2.536                    | 0.006              | 0.978                           |
|               | CCSDT            | 1.425              | 2.524                    | 0.006              | 0.958                           |
| d-aug-cc-pVTZ | CCSD             | 1.461              | 2.505                    | 0.006              | 0.987                           |
|               | CCSDT            | 1.437              | 2.491                    | 0.006              | 0.965                           |
| d-aug-cc-pVQZ | CCSD             | 1.468              | 2.500                    | 0.006              | 0.994                           |
| aug-cc-pVTZ   | TBE <sup>b</sup> | 1.438              | 2.498                    | 0.006              | 0.964                           |
| CBS           | TBE <sup>b</sup> | 1.44 ± 0.01        | 2.48 ± 0.01              | 0.006 ± 0.001      | 0.97 ± 0.01                     |
| lit.          | th.              | 1.426 <sup>c</sup> | 2.49 <sup>d</sup>        | 0.006 <sup>e</sup> |                                 |
|               | exp.             | 1.403 <sup>f</sup> | 2.14 <sup>g</sup>        |                    |                                 |

<sup>a</sup>We report the norm of the dipoles. See the caption of Table 1 for details. <sup>b</sup>See the corresponding footnotes in Table 7. <sup>c</sup>CISD value from ref 187. <sup>d</sup>exFCI/aug-cc-pVTZ transition energies corrected for basis set effects up to aug-cc-pV5Z from ref 8. <sup>e</sup>LR-CC3/aug-cc-pVTZ  $f$  from ref 8. <sup>f</sup>From Stark effect measurements (ref 186). <sup>g</sup>Experiment 0–0 energy from ref 189.

the CBS extrapolations come with small error bars. One notes that the geometrical relaxation of the ES increases the predicted dipole by *ca.* +0.11 D for all methods. Our TBE/CBS for  $\mu^{\text{GS}}$ , 1.69 ± 0.01 D, is slightly above the Hai and Head-Gordon value (1.654 D), but the two available experiments also show significant discrepancies (see bottom

of Table 10). For the vertical transition energy, our TBE/aug-cc-pVTZ is the same as the result of a CIPSI calculation performed with the same basis set and logically exceeds the experimental 0–0 energy. For the ES dipole, we are aware of two experiments,<sup>184,185</sup> but the former investigated  $\mu_a$  (one of the two dipole components) only. The most recent experiment



**Table 12.** GS Dipole Moment  $\mu^{\text{GS}}$ , Vertical Transition Energies  $\Delta E_{\text{vert}}$ , Oscillator Strengths  $f$ , and ES Dipole Moments  $\mu_{\text{vert}}^{\text{ES}}$  Determined for Silylidene (GS Geometry)<sup>a</sup>

| basis         | method           | <sup>1</sup> A <sub>1</sub> | <sup>1</sup> A <sub>2</sub> (Ryd) |                                 | <sup>1</sup> B <sub>2</sub> (Ryd) |                    |                                 |
|---------------|------------------|-----------------------------|-----------------------------------|---------------------------------|-----------------------------------|--------------------|---------------------------------|
|               |                  | $\mu^{\text{GS}}$           | $\Delta E_{\text{vert}}$          | $\mu_{\text{vert}}^{\text{ES}}$ | $\Delta E_{\text{vert}}$          | $f$                | $\mu_{\text{vert}}^{\text{ES}}$ |
| 6-31+G(d)     | CCSD             | 0.091                       | 2.254                             | -1.845                          | 3.966                             | 0.045              | -0.080                          |
|               | CCSDT            | 0.028                       | 2.107                             | -1.891                          | 3.874                             | 0.042              | -0.237                          |
|               | CCSDTQ           | 0.019                       | 2.101                             | -1.909                          | 3.876                             | 0.042              | -0.256                          |
|               | CCSDTQP          | 0.018                       | 2.101                             | -1.911                          | 3.877                             | 0.042              | -0.259                          |
| aug-cc-pVDZ   | CCSD             | 0.181                       | 2.289                             | -1.836                          | 3.875                             | 0.036              | 0.162                           |
|               | CCSDT            | 0.115                       | 2.146                             | -1.889                          | 3.795                             | 0.034              | 0.005                           |
|               | CCSDTQ           | 0.105                       | 2.140                             | -1.905                          | 3.798                             | 0.034              | -0.012                          |
| aug-cc-pVTZ   | CCSD             | 0.235                       | 2.286                             | -1.851                          | 3.877                             | 0.036              | 0.161                           |
|               | CCSDT            | 0.153                       | 2.128                             | -1.905                          | 3.779                             | 0.033              | -0.018                          |
| aug-cc-pVQZ   | CCSD             | 0.249                       | 2.301                             | -1.848                          | 3.891                             | 0.037              | 0.186                           |
|               | CCSDT            | 0.187                       | 2.290                             | -1.831                          | 3.876                             | 0.036              | 0.164                           |
| d-aug-cc-pVDZ | CCSD             | 0.121                       | 2.146                             | -1.885                          | 3.796                             | 0.034              | 0.007                           |
|               | CCSDT            | 0.121                       | 2.146                             | -1.885                          | 3.796                             | 0.034              | 0.007                           |
| d-aug-cc-pVTZ | CCSD             | 0.236                       | 2.287                             | -1.848                          | 3.877                             | 0.036              | 0.166                           |
|               | CCSDT            | 0.155                       | 2.130                             | -1.902                          | 3.779                             | 0.033              | -0.014                          |
| d-aug-cc-pVQZ | CCSD             | 0.249                       | 2.301                             | -1.847                          | 3.890                             | 0.037              | 0.186                           |
|               | CCSDT            | 0.155                       | 2.130                             | -1.902                          | 3.779                             | 0.033              | -0.014                          |
| aug-cc-pVTZ   | TBE <sup>b</sup> | 0.142                       | 2.122                             | -1.924                          | 3.783                             | 0.034              | -0.039                          |
| CBS           | TBE <sup>b</sup> | 0.16 ± 0.01                 | 2.15 ± 0.00                       | -1.92 ± 0.01                    | 3.81 ± 0.01                       | 0.034 ± 0.01       | 0.00 ± 0.04                     |
| lit.          | th.              | 0.144 <sup>c</sup>          | 2.12 <sup>d</sup>                 |                                 | 3.80 <sup>d</sup>                 | 0.033 <sup>e</sup> |                                 |
|               | exp.             |                             | 1.88 <sup>f</sup>                 |                                 | 3.63 <sup>g</sup>                 |                    |                                 |

<sup>a</sup>See the caption of Table 1 for details. <sup>b</sup>See the corresponding footnotes in Table 7. <sup>c</sup>CCSD(T)/cc-pVCQZ from ref 190. <sup>d</sup>exFCI/aug-cc-pVTZ transition energies corrected for basis set effects up to aug-cc-pV5Z from ref 8. <sup>e</sup>LR-CC3/aug-cc-pVTZ  $f$  from ref 8. <sup>f</sup>0–0 energy from ref 191. <sup>g</sup>0–0 energy from ref 192.

yields a total  $\mu^{\text{ES}}$  of  $1.69 \pm 0.01$  D,<sup>185</sup> which indicates a very slight increase as compared to the GS dipole. Our  $\mu_{\text{vert}}^{\text{ES}}$  ( $1.69 \pm 0.01$  D) and  $\mu_{\text{adia}}^{\text{ES}}$  ( $1.80 \pm 0.01$  D) values apparently slightly undershoots and overestimates the measured change of dipole moment. Again, the final call on the relative accuracy of theory and experiment is hard to make.

Table 11 provides the dipole moments, oscillator strength, and transition energies for the smallest halocarbene, HCF, a system isoelectronic to the previous one. Although we note a small oscillation of the GS dipole and transition energies going from CCSD to CCSDT and CCSDTQ, it is obvious that the convergence with respect to the CC order is fast. Likewise, basis set effects are moderate in the Dunning series, whereas the use of Pople's basis set yields grossly overestimated oscillator strengths and ES dipole moments. In short, reaching accurate values is not problematic. Our TBE/CBS for  $\mu^{\text{GS}}$ ,  $1.44 \pm 0.01$  D, is very close to an earlier CISD estimate,  $1.43$  D,<sup>187</sup> and both are slightly larger than the most recent measurement we are aware of ( $1.40$  D).<sup>188</sup> As for nitroxyl, our TBE for the vertical transition energy is equivalent to the result of a recent CIPSI calculation, and both are logically larger than the experimental 0–0 energy. The small oscillator strength determined here is also the same as our earlier CC3/aug-cc-pVTZ estimate. We could not find previous estimates of the ES dipole in the literature, and our calculations yield a decrease of ca. 50% as compared to the GS value, which is in contrast with very similar values obtained for the two states of HNO.

**3.9. Silylidene.** Let us finish our tour by considering silylidene,  $\text{H}_2\text{C}=\text{Si}$ , a small original molecule presenting two well-defined low-lying Rydberg ESs.<sup>191–193</sup> Our results are collected in Table 12. The values of  $\mu^{\text{GS}}$  are small in magnitude for all methods, and one notes that CCSD significantly overestimates the dipole, whereas one needs at least a triple- $\zeta$  basis set to obtain reasonable data. Our TBE of  $0.16$  D for the GS dipole is close to the only previous theoretical value we did

find.<sup>190</sup> There is, to the best of our knowledge, no experimental measurement available. The values of  $\Delta E_{\text{vert}}$  of the two lowest transitions are insensitive to the addition of quadruples in the CC series and they converge quite well with respect to the basis set size. The current TBEs are equal to the ones we obtained earlier applying a different strategy to reach the FCI limit<sup>7</sup> and they remain slightly larger than the experimental 0–0 energies.<sup>191,192</sup> For the two ESs, we disclose here the two first estimates of the dipole moments. For the lowest excitation, the dipole clearly flips direction as compared to the GS, which is in contrast with thioformaldehyde, and also becomes much larger than the GS dipole with a trustworthy TBE of  $-1.92 \pm 0.01$  D. For the second ES, all methods predict relatively small  $\mu_{\text{vert}}^{\text{ES}}$  values, with the CCSD and CCSDT signs sometimes in disagreement for a given basis set. Although the addition of a second set of diffuse orbitals has a quite small effect, the convergence with the size of the basis is quite slow, and we can only state that the final dipole should be almost null, although its sign remains unknown. Finally, one notes that 6-31+G(d) provides too large oscillator strengths for the second ES, but the stability is otherwise remarkable. One can likely be confident in the proposed TBE value ( $0.034$ ).

## 4. CONCLUSIONS

In this contribution, we have considered 30 singlet ESs in 13 small molecules and strived to obtain oscillator strengths and dipole moments as accurately as possible. To this end, we have performed a series of CC calculations going from (LR) CCSD to CCSDTQP using a large panel of basis sets containing one or two sets of diffuse functions. In all cases, we have obtained FCI/aug-cc-pVTZ quality properties and estimates of the corresponding FCI/CBS values, the latter coming with quite large uncertainties in some cases. Although FCI results do obviously yield rather definitive answers, we treated only small molecules here with computationally expensive methods, so

the transferability of this strategy to larger compounds is indeed limited. Regarding the CC expansion, we found that the correction brought by the P term is always negligible, whereas the impact of Q is often rather small, although some exceptions to the latter statement have been observed for the considered set. For instance, a reduction of the oscillator strength and ES dipole by  $-15\%$  and  $-0.40$  D, respectively, is observed for the valence  $\pi \rightarrow \pi^*$  transition of thioformaldehyde. More problematic is the convergence of the computed properties while increasing the size of the atomic basis set: this convergence can go from very smooth to erratic. For some states, huge differences between the results obtained with simply and doubly augmented basis sets are indeed found. The oscillator strengths determined for the three close-lying  $\Pi_u$  ESs of dinitrogen is a typical example of this problem caused by state mixing. All in all, when choices have to be made, it seems a better option to use CCSDT with a very large basis set rather than CCSDTQ with a smaller one when one wishes to perform comparisons with experiment, which as explained in the Introduction, is always a challenging task. We have also found several examples herein in which one property, for example, the oscillator strength, is rather independent of the selected basis set, whereas another, for example, the ES dipole, is not. One must therefore carefully check the basis set convergence and dependence for all considered states and properties.

Despite these challenges, it is certainly noteworthy that for the vast majority of the properties studied here, we could not only establish the most accurate theoretical estimates available to date but also obtain values that are compatible with the experimental knowledge when measurements are accessible, which is not always the case even for the small molecules considered here. Theory sometimes deliver smaller error bars than the corresponding experimental data. This is certainly the case for the smallest compounds treated here, for which very large basis sets could be employed. It should be stressed that the measurements of both  $f$  and  $\mu^{\text{ES}}$  are difficult, so depending on the experimental techniques, apparently incompatible results are quite commonly reported and the role of theory is likely critical. At this stage, it might be important to recall that we did not use any experimental input, as even our geometries are theoretically determined. The present effort is thus truly *ab initio*. However, it only provides an idealized picture as we did not aim at modeling vibronic effects.

As we expected at the beginning of the study, getting the right answer for the right reason in the context of ES properties is certainly more challenging than for the corresponding energies. It is therefore our hope that the reference values reported here will be useful benchmarks and will stimulate further studies in both the theoretical and experimental communities.

## ■ ASSOCIATED CONTENT

### SI Supporting Information

The Supporting Information is available free of charge at <https://pubs.acs.org/doi/10.1021/acs.jctc.0c01111>.

Extra data and Cartesian coordinates (PDF)

## ■ AUTHOR INFORMATION

### Corresponding Author

Denis Jacquemin – Université de Nantes, CNRS, CEISAM UMR 6230, F-44000 Nantes, France; [orcid.org/0000-0002-4217-0708](https://orcid.org/0000-0002-4217-0708); Email: [Denis.Jacquemin@univ-nantes.fr](mailto:Denis.Jacquemin@univ-nantes.fr)

## Authors

Amara Chrayteh – Université de Nantes, CNRS, CEISAM UMR 6230, F-44000 Nantes, France

Aymeric Blondel – Université de Nantes, CNRS, CEISAM UMR 6230, F-44000 Nantes, France

Pierre-François Loos – Laboratoire de Chimie et Physique Quantiques, Université de Toulouse, CNRS, UPS, 31062 Toulouse, France; [orcid.org/0000-0003-0598-7425](https://orcid.org/0000-0003-0598-7425)

Complete contact information is available at: <https://pubs.acs.org/10.1021/acs.jctc.0c01111>

## Notes

The authors declare no competing financial interest.

## ■ ACKNOWLEDGMENTS

A.C. and D.J. are indebted to the LumoMat program for support in the framework of the Fluo-34 grant. PFL thanks the Centre National de la Recherche Scientifique for funding. This research used resources of (i) the GENCI-TGCC (grant no. 2019-A0060801738); (ii) CALMIP under allocation 2020-18005 (Toulouse); (iii) CCIPL (Centre de Calcul Intensif des Pays de Loire); (iv) a local Troy cluster, and (v) HPC resources from ArronaxPlus (grant ANR-11-EQPX-0004 funded by the French National Agency for Research).

## ■ REFERENCES

- (1) Loos, P.-F.; Scemama, A.; Jacquemin, D. The Quest for Highly-Accurate Excitation Energies: A Computational Perspective. *J. Phys. Chem. Lett.* **2020**, *11*, 2374–2383.
- (2) Schreiber, M.; Silva-Junior, M. R.; Sauer, S. P. A.; Thiel, W. Benchmarks for Electronically Excited States: CASPT2, CC2, CCSD and CC3. *J. Chem. Phys.* **2008**, *128*, 134110.
- (3) Sauer, S. P. A.; Schreiber, M.; Silva-Junior, M. R.; Thiel, W. Benchmarks for Electronically Excited States: A Comparison of Noniterative and Iterative Triples Corrections in Linear Response Coupled Cluster Methods: CCSDR(3) versus CC3. *J. Chem. Theory Comput.* **2009**, *5*, 555–564.
- (4) Silva-Junior, M. R.; Schreiber, M.; Sauer, S. P. A.; Thiel, W. Benchmarks of Electronically Excited States: Basis Set Effects Benchmarks of Electronically Excited States: Basis Set Effects on CASPT2 Results. *J. Chem. Phys.* **2010**, *133*, 174318.
- (5) Loos, P.-F.; Scemama, A.; Blondel, A.; Garniron, Y.; Caffarel, M.; Jacquemin, D. A Mountaineering Strategy to Excited States: Highly-Accurate Reference Energies and Benchmarks. *J. Chem. Theory Comput.* **2018**, *14*, 4360–4379.
- (6) Loos, P.-F.; Boggio-Pasqua, M.; Scemama, A.; Caffarel, M.; Jacquemin, D. Reference Energies for Double Excitations. *J. Chem. Theory Comput.* **2019**, *15*, 1939–1956.
- (7) Loos, P.-F.; Lipparini, F.; Boggio-Pasqua, M.; Scemama, A.; Jacquemin, D. A Mountaineering Strategy to Excited States: Highly-Accurate Energies and Benchmarks for Medium Size Molecules. *J. Chem. Theory Comput.* **2020**, *16*, 1711–1741.
- (8) Loos, P.-F.; Scemama, A.; Boggio-Pasqua, M.; Jacquemin, D. A Mountaineering Strategy to Excited States: Highly-Accurate Energies and Benchmarks for Exotic Molecules and Radicals. *J. Chem. Theory Comput.* **2020**, *16*, 3720–3736.
- (9) Furche, F.; Ahlrichs, R. Adiabatic Time-Dependent Density Functional Methods for Excited States Properties. *J. Chem. Phys.* **2002**, *117*, 7433–7447.
- (10) Dierksen, M.; Grimme, S. The Vibronic Structure of Electronic Absorption Spectra of Large Molecules: A Time-Dependent Density Functional Study on the Influence of Exact Hartree-Fock Exchange. *J. Phys. Chem. A* **2004**, *108*, 10225–10237.
- (11) Hättig, C. *Response Theory and Molecular Properties (A Tribute to Jan Lindenberg and Poul Jørgensen)*; Jensen, H. A., Ed.; Advances in Quantum Chemistry; Academic Press, 2005; Vol. 50; pp 37–60.

- (12) Goerigk, L.; Moellmann, J.; Grimme, S. Computation of Accurate Excitation Energies for Large Organic Molecules with Double-Hybrid Density Functionals. *Phys. Chem. Chem. Phys.* **2009**, *11*, 4611–4620.
- (13) Goerigk, L.; Grimme, S. Assessment of TD-DFT Methods and of Various Spin Scaled CIS<sub>n</sub>D and CC2 Versions for the Treatment of Low-Lying Valence Excitations of Large Organic Dyes. *J. Chem. Phys.* **2010**, *132*, 184103.
- (14) Send, R.; Kühn, M.; Furche, F. Assessing Excited State Methods by Adiabatic Excitation Energies. *J. Chem. Theory Comput.* **2011**, *7*, 2376–2386.
- (15) Jacquemin, D.; Planchat, A.; Adamo, C.; Mennucci, B. A TD-DFT Assessment of Functionals for Optical 0-0 Transitions in Solvated Dyes. *J. Chem. Theory Comput.* **2012**, *8*, 2359–2372.
- (16) Winter, N. O. C.; Graf, N. K.; Leutwyler, S.; Hättig, C. Benchmarks for 0–0 Transitions of Aromatic Organic Molecules: DFT/B3LYP, ADC(2), CC2, SOS-CC2 and SCS-CC2 Compared to High-resolution Gas-Phase Data. *Phys. Chem. Chem. Phys.* **2013**, *15*, 6623–6630.
- (17) Fang, C.; Oruganti, B.; Durbeej, B. How Method-Dependent Are Calculated Differences Between Vertical, Adiabatic and 0-0 Excitation Energies? *J. Phys. Chem. A* **2014**, *118*, 4157–4171.
- (18) Jacquemin, D.; Duchemin, I.; Blase, X. 0–0 Energies Using Hybrid Schemes: Benchmarks of TD-DFT, CIS(D), ADC(2), CC2, and BSE/GW formalisms for 80 Real-Life Compounds. *J. Chem. Theory Comput.* **2015**, *11*, 5340–5359.
- (19) Oruganti, B.; Fang, C.; Durbeej, B. Assessment of a Composite CC2/DFT Procedure for Calculating 0–0 Excitation Energies of Organic Molecules. *Mol. Phys.* **2016**, *114*, 3448–3463.
- (20) Schwabe, T.; Goerigk, L. Time-Dependent Double-Hybrid Density Functionals with Spin-Component and Spin-Opposite Scaling. *J. Chem. Theory Comput.* **2017**, *13*, 4307–4323.
- (21) Loos, P.-F.; Galland, N.; Jacquemin, D. Theoretical 0–0 Energies with Chemical Accuracy. *J. Phys. Chem. Lett.* **2018**, *9*, 4646–4651.
- (22) Loos, P.-F.; Jacquemin, D. Chemically Accurate 0-0 Energies with not-so-Accurate Excited State Geometries. *J. Chem. Theory Comput.* **2019**, *15*, 2481–2491.
- (23) Loos, P. F.; Jacquemin, D. Evaluating 0-0 Energies with Theoretical Tools: a Short Review. *ChemPhotoChem* **2019**, *3*, 684–696.
- (24) Brémond, E.; Savarese, M.; Adamo, C.; Jacquemin, D. Accuracy of TD-DFT Geometries: a Fresh Look. *J. Chem. Theory Comput.* **2018**, *14*, 3715–3727.
- (25) Tajti, A.; Szalay, P. G. Accuracy of Spin-Component-Scaled CC2 Excitation Energies and Potential Energy Surfaces. *J. Chem. Theory Comput.* **2019**, *15*, 5523–5531.
- (26) Tajti, A.; Tulipán, L.; Szalay, P. G. Accuracy of Spin-Component Scaled ADC(2) Excitation Energies and Potential Energy Surfaces. *J. Chem. Theory Comput.* **2020**, *16*, 468–474.
- (27) Page, C. S.; Olivucci, M. Ground and Excited State CASPT2 Geometry Optimizations of Small Organic Molecules. *J. Comput. Chem.* **2003**, *24*, 298–309.
- (28) Bousquet, D.; Fukuda, R.; Maitarad, P.; Jacquemin, D.; Ciofini, I.; Adamo, C.; Ehara, M. Excited-State Geometries of Heteroaromatic Compounds: A Comparative TD-DFT and SAC-CI Study. *J. Chem. Theory Comput.* **2013**, *9*, 2368–2379.
- (29) Bousquet, D.; Fukuda, R.; Jacquemin, D.; Ciofini, I.; Adamo, C.; Ehara, M. Benchmark Study on the Triplet Excited-State Geometries and Phosphorescence Energies of Heterocyclic Compounds: Comparison Between TD-PBE0 and SAC-CI. *J. Chem. Theory Comput.* **2014**, *10*, 3969–3979.
- (30) Jagau, T.-C.; Gauss, J. Ground and Excited State Geometries via Mukherjee's Multireference Coupled-Cluster Method. *Chem. Phys.* **2012**, *401*, 73–87.
- (31) Guareschi, R.; Filippi, C. Ground- and Excited-State Geometry Optimization of Small Organic Molecules with Quantum Monte Carlo. *J. Chem. Theory Comput.* **2013**, *9*, 5513–5525.
- (32) Tuna, D.; Lu, Y.; Koslowski, A.; Thiel, W. Semiempirical Quantum-Chemical Orthogonalization-Corrected Methods: Benchmarks of Electronically Excited States. *J. Chem. Theory Comput.* **2016**, *12*, 4400–4422.
- (33) Budzák, Š.; Scalmani, G.; Jacquemin, D. Accurate Excited-State Geometries: a CASPT2 and Coupled-Cluster Reference Database for Small Molecules. *J. Chem. Theory Comput.* **2017**, *13*, 6237–6252.
- (34) Jacquemin, D. What is the Key for Accurate Absorption and Emission Calculations ? Energy or Geometry ? *J. Chem. Theory Comput.* **2018**, *14*, 1534–1543.
- (35) Fihey, A.; Jacquemin, D. Performances of Density Functional Tight-Binding Methods for Describing Ground and Excited State Geometries of Organic Molecules. *J. Chem. Theory Comput.* **2019**, *15*, 6267–6276.
- (36) Tajti, A.; Stanton, J. F.; Matthews, D. A.; Szalay, P. G. Accuracy of Coupled Cluster Excited State Potential Energy Surfaces. *J. Chem. Theory Comput.* **2018**, *14*, 5859–5869.
- (37) Gozem, S.; Schapiro, I.; Ferre, N.; Olivucci, M. The Molecular Mechanism of Thermal Noise in Rod Photoreceptors. *Science* **2012**, *337*, 1225–1228.
- (38) Tuna, D.; Lefrançois, D.; Wolański, Ł.; Gozem, S.; Schapiro, I.; Andruniów, T.; Dreuw, A.; Olivucci, M. Assessment of Approximate Coupled-Cluster and Algebraic-Diagrammatic-Construction Methods for Ground- and Excited-State Reaction Paths and the Conical-Intersection Seam of a Retinal-Chromophore Model. *J. Chem. Theory Comput.* **2015**, *11*, 5758–5781.
- (39) Kánnár, D.; Szalay, P. G. Benchmarking Coupled Cluster Methods on Valence Singlet Excited States. *J. Chem. Theory Comput.* **2014**, *10*, 3757–3765.
- (40) Robinson, D. Comparison of the Transition Dipole Moments Calculated by TDDFT with High Level Wave Function Theory. *J. Chem. Theory Comput.* **2018**, *14*, 5303–5309.
- (41) Caricato, M.; Trucks, G. W.; Frisch, M. J.; Wiberg, K. B. Oscillator Strength: How Does TDDFT Compare to EOM-CCSD? *J. Chem. Theory Comput.* **2010**, *7*, 456–466.
- (42) Li, Y.; Wan, J.; Xu, X. Theoretical Study of the Vertical Excited States of Benzene, Pyrimidine, and Pyrazine by the Symmetry Adapted Cluster – Configuration Interaction Method. *J. Comput. Chem.* **2007**, *28*, 1658–1667.
- (43) Silva-Junior, M. R.; Sauer, S. P. A.; Schreiber, M.; Thiel, W. Basis Set Effects on Coupled Cluster Benchmarks of Electronically Excited States: CC3, CCSDR(3) and CC2. *Mol. Phys.* **2010**, *108*, 453–465.
- (44) Jacquemin, D.; Duchemin, I.; Blondel, A.; Blase, X. Assessment of the Accuracy of the Bethe-Salpeter (BSE/GW) Oscillator Strengths. *J. Chem. Theory Comput.* **2016**, *12*, 3969–3981.
- (45) Hellweg, A. The Accuracy of Dipole Moments from Spin-Component Scaled CC2 in Ground and Electronically Excited States. *J. Chem. Phys.* **2011**, *134*, 064103.
- (46) Jacquemin, D. Excited-State Dipole and Quadrupole Moments: TD-DFT versus CC2. *J. Chem. Theory Comput.* **2016**, *12*, 3993–4003.
- (47) Hait, D.; Head-Gordon, M. How Accurate Is Density Functional Theory at Predicting Dipole Moments? An Assessment Using a New Database of 200 Benchmark Values. *J. Chem. Theory Comput.* **2018**, *14*, 1969–1981.
- (48) Borges, I. Influences on the Calculation of Accurate and Basis Set Extrapolated Oscillator Strengths: the A1B1←X1A1 Transition of H<sub>2</sub>O. *J. Phys. B: At, Mol. Opt. Phys.* **2006**, *39*, 641–650.
- (49) Nielsen, E. S.; Jorgensen, P.; Oddershede, J. Transition Moments and Dynamic Polarizabilities in a Second Order Polarization Propagator Approach. *J. Chem. Phys.* **1980**, *73*, 6238–6246.
- (50) Schmitt, M.; Meerts, L. *Frontiers and Advances in Molecular Spectroscopy*; Laane, J., Ed.; Elsevier, 2018; Chapter 5, pp 143–193.
- (51) Lombardi, J. R. On the Comparison of Solvatochromic Shifts with Gas Phase Stark Effect Measurements. *Spectrochim. Acta, Part A* **1987**, *43*, 1323–1324.
- (52) Eriksen, J. J.; Gauss, J. Many-Body Expanded Full Configuration Interaction. II. Strongly Correlated Regime. *J. Chem. Phys.* **2020**, *153*, 154107.

- (53) Christiansen, O.; Koch, H.; Jørgensen, P. Response Functions in the CC3 Iterative Triple Excitation Model. *J. Chem. Phys.* **1995**, *103*, 7429–7441.
- (54) Koch, H.; Christiansen, O.; Jørgensen, P.; Olsen, J. Excitation Energies of BH, CH<sub>2</sub> and Ne in Full Configuration Interaction and the Hierarchy CCS, CC2, CCSD and CC3 of Coupled Cluster Models. *Chem. Phys. Lett.* **1995**, *244*, 75–82.
- (55) Aidas, K.; Angeli, C.; Bak, K. L.; Bakken, V.; Bast, R.; Boman, L.; Christiansen, O.; Cimraglia, R.; Coriani, S.; Dahle, P.; Dalskov, E. K.; Ekström, U.; Enevoldsen, T.; Eriksen, J. J.; Ettenhuber, P.; Fernández, B.; Ferrighi, L.; Fliegl, H.; Frediani, L.; Hald, K.; Halkier, A.; Hättig, C.; Heiberg, H.; Helgaker, T.; Hennum, A. C.; Hettema, H.; Hjertenaes, E.; Host, S.; Høyvik, I.-M.; Iozzi, M. F.; Jansík, B.; Jensen, H. J. A.; Jonsson, D.; Jørgensen, P.; Kauczor, J.; Kirpekar, S.; Kjaergaard, T.; Klopper, W.; Knecht, S.; Kobayashi, R.; Koch, H.; Kongsted, J.; Krapp, A.; Kristensen, K.; Ligabue, A.; Lutnaes, O. B.; Melo, J. I.; Mikkelsen, K. V.; Myhre, R. H.; Neiss, C.; Nielsen, C. B.; Norman, P.; Olsen, J.; Olsen, J. M. H.; Osted, A.; Packer, M. J.; Pawłowski, F.; Pedersen, T. B.; Provasi, P. F.; Reine, S.; Rinkevicius, Z.; Ruden, T. A.; Ruud, K.; Rybkin, V. V.; Salek, P.; Samson, C. C. M.; de Merás, A. S.; Sauer, T.; Schimmelpennig, B.; Sneskov, K.; Steindal, A. H.; Sylvester-Hvid, K. O.; Taylor, P. R.; Teale, A. M.; Tellgren, E. I.; Tew, D. P.; Thorvaldsen, A. J.; Thøgersen, L.; Vahtras, O.; Watson, M. A.; Wilson, D. J. D.; Ziolkowski, M.; Ågren, H. The Dalton Quantum Chemistry Program System. *Wiley Interdiscip. Rev.: Comput. Mol. Sci.* **2014**, *4*, 269–284.
- (56) CFOUR, Coupled-Cluster techniques for Computational Chemistry, a quantum-chemical program package by Stanton, J. F.; Gauss, J.; Cheng, L.; Harding, M. E.; Matthews, D. A.; Szalay, P. G. with contributions from Auer, A. A.; Bartlett, R. J.; Benedikt, U.; Berger, C.; Bernholdt, D. E.; Bomble, Y. J.; Christiansen, O.; Engel, F.; Faber, R.; Heckert, M.; Heun, O.; Hilgenberg, C.; Huber, M.; Jagau, T.-C.; Jonsson, D.; Jusélius, J.; Kirsch, T.; Klein, K.; Lauderdale, W. J.; Lipparini, F.; Metzroth, T.; Mück, L. A.; O'Neill, D. P.; Price, D. R.; Prochnow, E.; Puzzarini, C.; Ruud, K.; Schiffmann, F.; Schwalbach, W.; Simmons, C.; Stopkowitz, S.; Tajti, A.; Vázquez, J.; Wang, F.; Watts, J. D. and the integral packages MOLECULE (Almlöf, J. and Taylor, P. R.), PROPS (Taylor, P. R.), ABACUS (Helgaker, T.; Aa Jensen, H.J.; Jørgensen, P.; Olsen, J.), and ECP routines by Mitin, A. V.; van Wüllen, C. For the current version, see <http://www.cfour.de>.
- (57) Helgaker, T.; Klopper, W.; Koch, H.; Noga, J. Basis-Set Convergence of Correlated Calculations on Water. *J. Chem. Phys.* **1997**, *106*, 9639–9646.
- (58) Halkier, A.; Klopper, W.; Helgaker, T.; Jørgensen, P. Basis-set Convergence of the Molecular Electric Dipole Moment. *J. Chem. Phys.* **1999**, *111*, 4424–4430.
- (59) Kállay, M.; Nagy, P. R.; Mester, D.; Rolik, Z.; Samu, G.; Csontos, J.; Csóka, J.; Szabó, P. B.; Gyevi-Nagy, L.; Hégyel, B.; Ladjanszki, I.; Szegedy, L.; Ladóczki, B.; Petrov, K.; Farkas, M.; Mezei, P. D.; Ganyecz, Á. The MRCC Program System: Accurate Quantum Chemistry from Water to Proteins. *J. Chem. Phys.* **2020**, *152*, 074107.
- (60) Kállay, M.; Rolik, Z.; Csontos, J.; Nagy, P.; Samu, G.; Mester, D.; Csóka, J.; Szabó, B.; Ladjanszki, I.; Szegedy, L.; Ladóczki, B.; Petrov, K.; Farkas, M.; Mezei, P. D.; Hégyel, B. MRCC, *Quantum Chemical Program*, 2017; see: [www.mrcc.hu](http://www.mrcc.hu).
- (61) Purvis, G. D., III; Bartlett, R. J. A Full Coupled-Cluster Singles and Doubles Model: The Inclusion of Disconnected Triples. *J. Chem. Phys.* **1982**, *76*, 1910–1918.
- (62) Scuseria, G. E.; Scheiner, A. C.; Lee, T. J.; Rice, J. E.; Schaefer, H. F. The Closed-Shell Coupled Cluster Single and Double Excitation (CCSD) Model for the Description of Electron Correlation. A Comparison with Configuration Interaction (CISD) Results. *J. Chem. Phys.* **1987**, *86*, 2881–2890.
- (63) Koch, H.; Jensen, H. J. r. a.; Jørgensen, P.; Helgaker, T. Excitation Energies from the Coupled Cluster Singles and Doubles Linear Response Function (CCSDLR). Applications to Be, CH<sup>+</sup>, CO, and H<sub>2</sub>O. *J. Chem. Phys.* **1990**, *93*, 3345–3350.
- (64) Stanton, J. F.; Bartlett, R. J. The Equation of Motion Coupled-Cluster Method - A Systematic Biorthogonal Approach to Molecular Excitation Energies, Transition-Probabilities, and Excited-State Properties. *J. Chem. Phys.* **1993**, *98*, 7029–7039.
- (65) Stanton, J. F. Many-Body Methods for Excited State Potential Energy Surfaces. I: General Theory of Energy Gradients for the Equation-of-Motion Coupled-Cluster Method. *J. Chem. Phys.* **1993**, *99*, 8840–8847.
- (66) Noga, J.; Bartlett, R. J. The Full CCSDT Model for Molecular Electronic Structure. *J. Chem. Phys.* **1987**, *86*, 7041–7050.
- (67) Scuseria, G. E.; Schaefer, H. F. A New Implementation of the Full CCSDT Model for Molecular Electronic Structure. *Chem. Phys. Lett.* **1988**, *152*, 382–386.
- (68) Kucharski, S. A.; Wloch, M.; Musiał, M.; Bartlett, R. J. Coupled-Cluster Theory for Excited Electronic States: The Full Equation-Of-Motion Coupled-Cluster Single, Double, and Triple Excitation Method. *J. Chem. Phys.* **2001**, *115*, 8263–8266.
- (69) Kowalski, K.; Piecuch, P. The Active-Space Equation-of-Motion Coupled-Cluster Methods for Excited Electronic States: Full EOMCCSDt. *J. Chem. Phys.* **2001**, *115*, 643–651.
- (70) Kowalski, K.; Piecuch, P. Excited-State Potential Energy Curves of CH<sup>+</sup>: a Comparison of the EOMCCSDt And Full EOMCCSDT Results. *Chem. Phys. Lett.* **2001**, *347*, 237–246.
- (71) Kucharski, S. A.; Bartlett, R. J. Recursive Intermediate Factorization and Complete Computational Linearization of the Coupled-Cluster Single, Double, Triple, and Quadruple Excitation Equations. *Theor. Chim. Acta* **1991**, *80*, 387–405.
- (72) Kállay, M.; Gauss, J.; Szalay, P. G. Analytic First Derivatives for General Coupled-Cluster and Configuration Interaction Models. *J. Chem. Phys.* **2003**, *119*, 2991–3004.
- (73) Kállay, M.; Gauss, J. Calculation of Excited-State Properties Using General Coupled-Cluster and Configuration-Interaction Models. *J. Chem. Phys.* **2004**, *121*, 9257–9269.
- (74) Hirata, S. Higher-Order Equation-of-Motion Coupled-Cluster Methods. *J. Chem. Phys.* **2004**, *121*, 51–59.
- (75) Suellen, C.; Freitas, R. G.; Loos, P.-F.; Jacquemin, D. Cross Comparisons Between Experiment, TD-DFT, CC, and ADC for Transition Energies. *J. Chem. Theory Comput.* **2019**, *15*, 4581–4590.
- (76) Frisch, M. J.; Trucks, G. W.; Schlegel, H. B.; Scuseria, G. E.; Robb, M. A.; Cheeseman, J. R.; Scalmani, G.; Barone, V.; Petersson, G. A.; Nakatsuji, H.; Li, X.; Caricato, M.; Marenich, A. V.; Bloino, J.; Janesko, B. G.; Gomperts, R.; Mennucci, B.; Hratchian, H. P.; Ortiz, J. V.; Izmaylov, A. F.; Sonnenberg, J. L.; Williams-Young, D.; Ding, F.; Lipparini, F.; Egidi, F.; Goings, J.; Peng, B.; Petrone, A.; Henderson, T.; Ranasinghe, D.; Zakrzewski, V. G.; Gao, J.; Rega, N.; Zheng, G.; Liang, W.; Hada, M.; Ehara, M.; Toyota, K.; Fukuda, R.; Hasegawa, J.; Ishida, M.; Nakajima, T.; Honda, Y.; Kitao, O.; Nakai, H.; Vreven, T.; Throssell, K.; Montgomery, J. A., Jr.; Peralta, J. E.; Ogliaro, F.; Bearpark, M. J.; Heyd, J. J.; Brothers, E. N.; Kudin, K. N.; Staroverov, V. N.; Keith, T. A.; Kobayashi, R.; Normand, J.; Raghavachari, K.; Rendell, A. P.; Burant, J. C.; Iyengar, S. S.; Tomasi, J.; Cossi, M.; Millam, J. M.; Klene, M.; Adamo, C.; Cammi, R.; Ochterski, J. W.; Martin, R. L.; Morokuma, K.; Farkas, O.; Foresman, J. B.; Fox, D. J. *Gaussian 16*, Revision A.03; Gaussian Inc: Wallingford CT, 2016.
- (77) Krylov, A. I.; Gill, P. M. W. Q-Chem: an Engine for Innovation. *Wiley Interdiscip. Rev.: Comput. Mol. Sci.* **2013**, *3*, 317–326.
- (78) Folkestad, S. D.; Kjønstad, E. F.; Myhre, R. H.; Andersen, J. H.; Balbi, A.; Coriani, S.; Giovannini, T.; Goletto, T.; Haugland, T. S.; Hutcheson, A.; Høyvik, I.-M.; Moitra, T.; Paul, A. C.; Scavino, M.; Skeidsvoll, A. S.; Tveten, Å. H.; Koch, H. eT 1.0: An Open Source Electronic Structure Program with Emphasis on Coupled Cluster and Multilevel Methods. *J. Chem. Phys.* **2020**, *152*, 184103.
- (79) Koch, H.; Jørgensen, P. Coupled Cluster Response Functions. *J. Chem. Phys.* **1990**, *93*, 3333–3344.
- (80) Christiansen, O.; Jørgensen, P.; Hättig, C. Response Functions from Fourier Component Variational Perturbation Theory Applied to a Time-Averaged Quasienergy. *Int. J. Quantum Chem.* **1998**, *68*, 1–52.
- (81) Caricato, M.; Trucks, G. W.; Frisch, M. J. On the Difference Between the Transition Properties Calculated with Linear Response-

and Equation of Motion-CCSD Approaches. *J. Chem. Phys.* **2009**, *131*, 174104.

(82) Pawłowski, F.; Jørgensen, P.; Hättig, C. Gauge Invariance of Oscillator Strengths in the Approximate Coupled Cluster Triples Model CC3. *Chem. Phys. Lett.* **2004**, *389*, 413–420.

(83) Trucks, G. W.; Salter, E. A.; Sosa, C.; Bartlett, R. J. Theory and Implementation of the MBPT Density Matrix. An Application to One-Electron Properties. *Chem. Phys. Lett.* **1988**, *147*, 359–366.

(84) Christiansen, O.; Koch, H.; Jørgensen, P. The Second-Order Approximate Coupled Cluster Singles and Doubles Model CC2. *Chem. Phys. Lett.* **1995**, *243*, 409–418.

(85) Balabanov, N. B.; Peterson, K. A. Basis set Limit Electronic Excitation Energies, Ionization Potentials, and Electron Affinities for the 3d Transition Metal Atoms: Coupled Cluster and Multireference Methods. *J. Chem. Phys.* **2006**, *125*, 074110.

(86) Kamiya, M.; Hirata, S. Higher-Order Equation-of-Motion Coupled-Cluster Methods for Ionization Processes. *J. Chem. Phys.* **2006**, *125*, 074111.

(87) Watson, M. A.; Chan, G. K.-L. Excited States of Butadiene to Chemical Accuracy: Reconciling Theory and Experiment. *J. Chem. Theory Comput.* **2012**, *8*, 4013–4018.

(88) Feller, D.; Peterson, K. A.; Davidson, E. R. A Systematic Approach to Vertically Excited States of Ethylene Using Configuration Interaction and Coupled Cluster Techniques. *J. Chem. Phys.* **2014**, *141*, 104302.

(89) Franke, P. R.; Moore, K. B.; Schaefer, H. F.; Douberly, G. E. tert-Butyl Peroxy Radical: Ground and First Excited State Energetics and Fundamental Frequencies. *Phys. Chem. Chem. Phys.* **2019**, *21*, 9747–9758.

(90) Koput, J. Ab Initio Spectroscopic Characterization of Borane, BH, in its  $X^1\Sigma^+$  Electronic State. *J. Comput. Chem.* **2015**, *36*, 2219–2227.

(91) Engin, S.; Sisourat, N.; Carniato, S. Ab initio Study of Low-Lying Excited States of HCl: Accurate Calculations of Optical Valence-Shell Excitations. *J. Chem. Phys.* **2012**, *137*, 154304.

(92) Thomson, R.; Dalby, F. W. An Experimental Determination of the Dipole Moments of the  $X(^1\Sigma)$  and  $A(^1\Pi)$  States of the BH Molecule. *Can. J. Phys.* **1969**, *47*, 1155–1158.

(93) Douglass, C. H.; Nelson, H. H.; Rice, J. K. Spectra, Radiative Lifetimes, and Band Oscillator Strengths of the  $A^1\Pi - X^1\Sigma^+$  Transition of BH. *J. Chem. Phys.* **1989**, *90*, 6940–6948.

(94) Dufayard, J.; Nedelec, O. Lifetime of the BH  $A^1\Pi$  State Excited by a Pulsed Dye Laser. *J. Chem. Phys.* **1978**, *69*, 4708–4709.

(95) Cheng, B.-M.; Chung, C.-Y.; Bahou, M.; Lee, Y.-P.; Lee, L. C. Quantitative Spectral Analysis of HCl and DCl in 120–220 nm: Effects of Singlet–Triplet Mixing. *J. Chem. Phys.* **2002**, *117*, 4293–4298.

(96) Li, W.-B.; Zhu, L.-F.; Yuan, Z.-S.; Liu, X.-J.; Xu, K.-Z. Optical Oscillator Strengths for Valence-Shell and Br-3d Inner-Shell Excitations of HCl and HBr. *J. Chem. Phys.* **2006**, *125*, 154310.

(97) Xu, Y.-C.; Liu, Y.-W.; Du, X.-J.; Xu, L.-Q.; Zhu, L.-F. Oscillator Strengths and Integral Cross Sections of the Valence-Shell Excitations of HCl Studied by Fast Electron Scattering. *Phys. Chem. Chem. Phys.* **2019**, *21*, 17433–17440.

(98) Lu, S.-I. Performance of Ornstein–Uhlenbeck Diffusion Quantum Monte Carlo for First-Row Diatomic Dissociation Energies and Dipole Moments. *J. Chem. Phys.* **2003**, *118*, 6152–6156.

(99) Páleniková, J.; Kraus, M.; Neogrády, P.; Kellö, V.; Urban, M. Theoretical Study of Molecular Properties of Low-Lying Electronic Excited States of H<sub>2</sub>O and H<sub>2</sub>S. *Mol. Phys.* **2008**, *106*, 2333–2344.

(100) Borges, I. Configuration Interaction Oscillator Strengths of the H<sub>2</sub>O Molecule: Transitions from the Ground to the B1A1, C1B1, D1A1, and  $1^4B_2$  Excited States. *Chem. Phys.* **2006**, *328*, 284–290.

(101) John, I. G.; Bacskay, G. B.; Hush, N. S. Finite Field Method Calculations. VI. Raman Scattering Activities, Infrared Absorption Intensities and Higher-Order Moments: SCF and CI Calculations for the Isotopic Derivatives of H<sub>2</sub>O and SCF Calculations for CH<sub>4</sub>. *Chem. Phys.* **1980**, *51*, 49–60.

(102) Ralphs, K.; Serna, G.; Hargreaves, L. R.; Khakoo, M. A.; Winstead, C.; McKoy, V. Excitation of the Six Lowest Electronic Transitions in Water by 9–20 eV Electrons. *J. Phys. B* **2013**, *46*, 125201.

(103) Thorn, P. A.; Brunger, M. J.; Teubner, P. J. O.; Diakomichalis, N.; Maddern, T.; Bolorizadeh, M. A.; Newell, W. R.; Kato, H.; Hoshino, M.; Tanaka, H.; Cho, H.; Kim, Y.-K. Cross Sections and Oscillator Strengths for Electron-Impact Excitation of the A1B1 Electronic State of Water. *J. Chem. Phys.* **2007**, *126*, 064306.

(104) Mota, R.; Parafita, R.; Giuliani, A.; Hubin-Franskin, M.-J.; Lourenço, J. M. C.; Garcia, G.; Hoffmann, S. V.; Mason, N. J.; Ribeiro, P. A.; Raposo, M.; Limão-Vieira, P. Water VUV Electronic State Spectroscopy by Synchrotron Radiation. *Chem. Phys. Lett.* **2005**, *416*, 152–159.

(105) Ertan, E.; Lundberg, M.; Sørensen, L. K.; Odelius, M. Setting the Stage for Theoretical X-Ray Spectra of the H<sub>2</sub>S Molecule with Multi-Configurational Quantum Chemical Calculations of the Energy Landscape. *J. Chem. Phys.* **2020**, *152*, 094305.

(106) Huiszoon, C.; Dymanus, A. Stark Effect of Millimeter Wave Transitions: I. Hydrogen Sulfide. *Physica* **1965**, *31*, 1049–1052.

(107) Masuko, H.; Morioka, Y.; Nakamura, M.; Ishiguro, E.; Sasanuma, M. Absorption Spectrum of the H<sub>2</sub>S Molecule In The Vacuum Ultraviolet Region. *Can. J. Phys.* **1979**, *57*, 745–760.

(108) Lee, L. C.; Wang, X.; Suto, M. Quantitative Photoabsorption and Fluorescence Spectroscopy of H<sub>2</sub>S and D<sub>2</sub>S at 49–240 nm. *J. Chem. Phys.* **1987**, *86*, 4353–4361.

(109) Feng, R.; Cooper, G.; Brion, C. E. Absolute Oscillator Strengths for Hydrogen Sulphide: I. Photoabsorption in the Valence-Shell and the S2p and 2s Inner-Shell Regions (4–260 eV). *Chem. Phys.* **1999**, *244*, 127–142.

(110) Pericou-Cayere, M.; Gelize, M.; Dargelos, A. Ab initio Calculations of Electronic Spectra of H<sub>2</sub>S and H<sub>2</sub>S<sub>2</sub>. *Chem. Phys.* **1997**, *214*, 81–89.

(111) Rauk, A.; Collins, S. The Ground and Excited States of Hydrogen Sulfide, Methanethiol, and Hydrogen Selenide. *J. Mol. Spectrosc.* **1984**, *105*, 438–452.

(112) Lovas, F. J.; Johnson, D. R. Microwave Spectrum of BF. *J. Chem. Phys.* **1971**, *55*, 41–44.

(113) Honigmann, M.; Hirsch, G.; Bunker, R. J. Theoretical Study of the Optical and Generalized Oscillator Strengths for Transitions Between Low-Lying Electronic States of the BF Molecule. *Chem. Phys.* **1993**, *172*, 59–71.

(114) Magoulas, I.; Kalemios, A.; Mavridis, A. An ab initio Study of the Electronic Structure of BF and BF<sup>+</sup>. *J. Chem. Phys.* **2013**, *138*, 104312.

(115) Mérawa, M.; Bégué, D.; Rérat, M.; Pouchan, C. Dynamic Polarizability and Hyperpolarizability for the 14 Electron Molecules CO and BF. *Chem. Phys. Lett.* **1997**, *280*, 203–211.

(116) Huber, K. P.; Herzberg, G. *Constants of Atomic Molecules; Molecular Spectra and Molecular Structure*; Van Nostrand: Princeton, 1979; Vol. 4.

(117) Coe, J. P.; Taylor, D. J.; Paterson, M. J. Monte Carlo Configuration Interaction Applied to Multipole Moments, Ionization Energies, and Electron Affinities. *J. Comput. Chem.* **2013**, *34*, 1083–1093.

(118) Cooper, D. L.; Kirby, K. Theoretical Study of Low Lying  $^1\Sigma^+$  and  $^1\Pi$  States of CO. I. Potential Energy Curves and Dipole Moments. *J. Chem. Phys.* **1987**, *87*, 424–432.

(119) Chan, W. F.; Cooper, G.; Brion, C. E. Absolute Optical Oscillator Strengths for Discrete and Continuum Photoabsorption of Carbon Monoxide (7–200 eV) and Transition Moments for the  $X^1\Sigma^+ \rightarrow A^1\Pi$  System. *Chem. Phys.* **1993**, *170*, 123–138.

(120) Fisher, N. J.; Dalby, F. W. On the Dipole Moments of Excited Singlet States of Carbon Monoxide. *Can. J. Phys.* **1976**, *54*, 258–261.

(121) Kang, X.; Liu, Y. W.; Xu, L. Q.; Ni, D. D.; Yang, K.; Hiraoka, N.; Tsuei, K. D.; Zhu, L. F. Oscillator Strength Measurement for the A(0–6) – X(0), C(0) – X(0), and E(0) – X(0) Transitions of CO by the Dipole ( $\gamma$ ,  $\gamma$ ) Method. *Astrophys. J.* **2015**, *807*, 96.

- (122) Drabbels, M.; Meerts, W. L.; ter Meulen, J. J. Determination of Electric Dipole Moments and Transition Probabilities of Low-Lying Singlet States of CO. *J. Chem. Phys.* **1993**, *99*, 2352–2358.
- (123) Scuseria, G. E.; Miller, M. D.; Jensen, F.; Geertsen, J. The Dipole Moment of Carbon Monoxide. *J. Chem. Phys.* **1991**, *94*, 6660–6663.
- (124) Nielsen, E. S.; Jorgensen, P.; Oddershede, J. *J. Chem. Phys.* **1980**, *22*, 1539–1548.
- (125) Carlson, T. A.; Đurić, N.; Erman, P.; Larsson, M. Correlation Between Perturbation and Collisional Transfers In The A, B, C and b States of CO as Revealed by High Resolution Lifetime Measurements. *Z. Phys. A* **1978**, *287*, 123–136.
- (126) Rocha, A. B.; Borges, I.; Bielschowsky, C. E. Optical and Generalized Oscillator Strengths for the  $B^1\Sigma^+$ ,  $C^1\Sigma^+$ , and  $E^1\Pi$  Vibronic Bands in the CO Molecule. *Phys. Rev. A* **1998**, *57*, 4394–4400.
- (127) Oddershede, J.; Grüner, N. E.; Diercksen, G. H. F. Comparison Between Equation of Motion and Polarization Propagator Calculations. *Chem. Phys.* **1985**, *97*, 303–310.
- (128) Neugebauer, J.; Baerends, E. J.; Nooijen, M. Vibronic Coupling and Double Excitations in Linear Response Time-Dependent Density Functional Calculations: Dipole-Allowed States of  $N_2$ . *J. Chem. Phys.* **2004**, *121*, 6155–6166.
- (129) Chan, W. F.; Cooper, G.; Sodhi, R. N. S.; Brion, C. E. Absolute Optical Oscillator Strengths for Discrete and Continuum Photoabsorption of Molecular Nitrogen (11–200 eV). *Chem. Phys.* **1993**, *170*, 81–97.
- (130) Ben-Shlomo, S. B.; Kaldor, U.  $N_2$  Excitations Below 15 eV by the Multireference Coupled-Cluster Method. *J. Chem. Phys.* **1990**, *92*, 3680–3682.
- (131) Ajello, J. M.; James, G. K.; Franklin, B. O.; Shemansky, D. E. Medium-Resolution Studies of Extreme Ultraviolet Emission from  $N_2$  by Electron Impact: Vibrational Perturbations and Cross Sections of the  $c^4'1\Sigma_u$  and  $b^1\Sigma_u$  states. *Phys. Rev. A* **1989**, *40*, 3524–3556.
- (132) The first, second, and third  $\Pi_u$  transitions have as largest MO contribution,  $A_g \rightarrow B_{2u}$ ,  $B_{1u} \rightarrow B_{3g}$  and  $B_{2u} \rightarrow A_g$  excitation, respectively, within the commonly used  $D_{2h}$  point group. There is nevertheless significant mixing, and we used the largest coefficient to discriminate the various  $\Pi_u$ .
- (133) Liu, Y.-W.; Kang, X.; Xu, L.-Q.; Ni, D.-D.; Yang, K.; Hiraoka, N.; Tsuei, K.-D.; Zhu, L.-F. Oscillator Strengths of Vibronic Excitations of Nitrogen Determined by the Dipole ( $\gamma$ ,  $\gamma$ ) Method. *Astrophys. J.* **2016**, *819*, 142.
- (134) Lavín, C.; Velasco, A.; Martín, I.; Bustos, E. MQDO Oscillator Strengths and Emission Coefficients for Electronic Transitions in  $N_2$  and NO. *Chem. Phys. Lett.* **2004**, *394*, 114–119.
- (135) Robin, M. B. *Higher Excited States of Polyatomic Molecules*; Robin, M. B., Ed.; Academic Press, 1985; Vol. III.
- (136) Serrano-Andrés, L.; Mechán, M.; Nebot-Gil, I.; Lindh, R.; Roos, B. O. Towards an Accurate Molecular Orbital Theory for Excited States: Ethene, Butadiene, and Hexatriene. *J. Chem. Phys.* **1993**, *98*, 3151–3162.
- (137) Merer, A. J.; Mulliken, R. S. Ultraviolet Spectra and Excited States of Ethylene and its Alkyl Derivatives. *Chem. Rev.* **1969**, *69*, 639–656.
- (138) Zelikoff, M.; Watanabe, K. Absorption Coefficients of Ethylene in the Vacuum Ultraviolet. *J. Opt. Soc. Am.* **1953**, *43*, 756–759.
- (139) Watts, J. D.; Gwaltney, S. R.; Bartlett, R. J. Coupled-Cluster Calculations of the Excitation Energies of Ethylene, Butadiene, and Cyclopentadiene. *J. Chem. Phys.* **1996**, *105*, 6979–6988.
- (140) Cooper, G.; Olney, T. N.; Brion, C. E. Absolute UV and Soft X-ray Photoabsorption of Ethylene by High Resolution Dipole (e,e) Spectroscopy. *Chem. Phys.* **1995**, *194*, 175–184.
- (141) Hammond, V. J.; Price, W. C. Oscillator Strengths of the Vacuum Ultra-Violet Absorption Bands of Benzene and Ethylene. *Trans. Faraday Soc.* **1955**, *51*, 605–610.
- (142) Foresman, J. B.; Head-Gordon, M.; Pople, J. A.; Frisch, M. J. Toward a Systematic Molecular Orbital Theory for Excited States. *J. Phys. Chem.* **1992**, *96*, 135–149.
- (143) Hadad, C. M.; Foresman, J. B.; Wiberg, K. B. Excited States of Carbonyl Compounds. 1. Formaldehyde and Acetaldehyde. *J. Phys. Chem.* **1993**, *97*, 4293–4312.
- (144) Head-Gordon, M.; Rico, R. J.; Oumi, M.; Lee, T. J. A Doubles Correction to Electronic Excited States From Configuration Interaction in the Space of Single Substitutions. *Chem. Phys. Lett.* **1994**, *219*, 21–29.
- (145) Head-Gordon, M.; Maurice, D.; Oumi, M. A Perturbative Correction to Restricted Open-Shell Configuration-Interaction with Single Substitutions for Excited-States of Radicals. *Chem. Phys. Lett.* **1995**, *246*, 114–121.
- (146) Gwaltney, S. R.; Bartlett, R. J. An Application of the Equation-Of-Motion Coupled Cluster Method to the Excited States of Formaldehyde, Acetaldehyde, and Acetone. *Chem. Phys. Lett.* **1995**, *241*, 26–32.
- (147) Wiberg, K. B.; Stratmann, R. E.; Frisch, M. J. A Time-Dependent Density Functional Theory Study of the Electronically Excited States of Formaldehyde, Acetaldehyde and Acetone. *Chem. Phys. Lett.* **1998**, *297*, 60–64.
- (148) Wilberg, K. B.; de Oliveira, A. E.; Trucks, G. A Comparison of the Electronic Transition Energies for Ethene, Isobutene, Formaldehyde, and Acetone Calculated Using RPA, TDDFT, and EOM-CCSD. Effect of Basis Sets. *J. Phys. Chem. A* **2002**, *106*, 4192–4199.
- (149) Peach, M. J. G.; Benfield, P.; Helgaker, T.; Tozer, D. J. Excitation Energies in Density Functional Theory: an Evaluation and a Diagnostic Test. *J. Chem. Phys.* **2008**, *128*, 044118.
- (150) Shen, J.; Li, S. Block Correlated Coupled Cluster Method with the Complete Active-Space Self-Consistent-Field Reference Function: Applications for Low-Lying Electronic Excited States. *J. Chem. Phys.* **2009**, *131*, 174101.
- (151) Caricato, M.; Trucks, G. W.; Frisch, M. J.; Wiberg, K. B. Electronic Transition Energies: A Study of the Performance of a Large Range of Single Reference Density Functional and Wave Function Methods on Valence and Rydberg States Compared to Experiment. *J. Chem. Theory Comput.* **2010**, *6*, 370–383.
- (152) Li, X.; Paldus, J. Multi-Reference State-Universal Coupled-Cluster Approaches to Electronically Excited States. *J. Chem. Phys.* **2011**, *134*, 214118.
- (153) Leang, S. S.; Zahariev, F.; Gordon, M. S. Benchmarking the Performance of Time-Dependent Density Functional Methods. *J. Chem. Phys.* **2012**, *136*, 104101.
- (154) Hoyer, C. E.; Ghosh, S.; Truhlar, D. G.; Gagliardi, L. Multiconfiguration Pair-Density Functional Theory Is as Accurate as CASPT2 for Electronic Excitation. *J. Phys. Chem. Lett.* **2016**, *7*, 586–591.
- (155) Kánnár, D.; Tajti, A.; Szalay, P. G. Accuracy of Coupled Cluster Excitation Energies in Diffuse Basis Sets. *J. Chem. Theory Comput.* **2017**, *13*, 202–209.
- (156) Müller, T.; Lischka, H. Simultaneous Calculation of Rydberg and Valence Excited States of Formaldehyde. *Theor. Chem. Acc.* **2001**, *106*, 369–378.
- (157) Hachey, M.; Bruna, P. J.; Grein, F. Configuration Interaction Studies on the  $S_2$  Surface of  $H_2CO$ :  $2^1A'$  ( $\sigma$ ,  $\pi^*/\pi$ ,  $\pi^*$ ) as Perturber of  $1^1B_2(n, 3s)$ . *J. Chem. Soc., Faraday Trans.* **1994**, *90*, 683–688.
- (158) Gómez-Carrasco, S.; Müller, T.; Köppel, H. Ab Initio Study of the VUV-Induced Multistate Photodynamics of Formaldehyde. *J. Phys. Chem. A* **2010**, *114*, 11436–11449.
- (159) Fabricant, B.; Krieger, D.; Muentner, J. S. Molecular Beam Electric Resonance Study of Formaldehyde, Thioformaldehyde, and Ketene. *J. Chem. Phys.* **1977**, *67*, 1576–1586.
- (160) Haner, D. A.; Dows, D. A. Electric-Field-Induced Spectra: Excited-State Dipole Moment from Line-Shape Analysis. *J. Chem. Phys.* **1968**, *49*, 601–605.
- (161) Weiss, M. J.; Kuyatt, C. E.; Mielczarek, S. Inelastic Electron Scattering from Formaldehyde. *J. Chem. Phys.* **1971**, *54*, 4147–4150.

- (162) Causley, G. C.; Russell, B. R. Electric Dipole Moment and Polarizability of the 1749 Å,  $^1B_2$  Excited State of Formaldehyde. *J. Chem. Phys.* **1978**, *68*, 3797–3800.
- (163) Causley, G. C.; Russell, B. R. Electric Dichroism Spectroscopy in the Vacuum Ultraviolet. 2. Formaldehyde, Acetaldehyde, and Acetone. *J. Am. Chem. Soc.* **1979**, *101*, 5573–5578.
- (164) Vaccaro, P. H.; Zabludoff, A.; Carrera-Patiño, M. E.; Kinsey, J. L.; Field, R. W. High Precision Dipole Moments in A1A2 Formaldehyde Determined via Stark Quantum Beat Spectroscopy. *J. Chem. Phys.* **1989**, *90*, 4150–4167.
- (165) Cooper, G.; Anderson, J. E.; Brion, C. E. Absolute Photoabsorption and Photoionization of Formaldehyde in the VUV and Soft X-ray Regions (3–200 eV). *Chem. Phys.* **1996**, *209*, 61–77.
- (166) Benková, Z.; Čerušák, I.; Zahradník, P. Electric Properties of Formaldehyde, Thioformaldehyde, Urea, Formamide, and Thioformamide – Post-HF and DFT Study. *Int. J. Quantum Chem.* **2007**, *107*, 2133–2152.
- (167) Clouthier, D. J.; Ramsay, D. A. The Spectroscopy of Formaldehyde and Thioformaldehyde. *Annu. Rev. Phys. Chem.* **1983**, *34*, 31–58.
- (168) Suzuki, T.; Saito, S.; Hirota, E. Dipole Moments of  $H_2CS$  in the A1A2( $\nu=0$ ) and Sa3A2( $\nu_3=1$ ) States by MODR Spectroscopy. *J. Mol. Spectrosc.* **1985**, *111*, 54–61.
- (169) Goetz, W.; Moule, D. C.; Ramsay, D. A. The Electric Dipole Moment of the C1B2( $3s \leftarrow n$ ) State of Thioformaldehyde. *Can. J. Phys.* **1981**, *59*, 1635–1639.
- (170) Johnson, D. R.; Powell, F. X.; Kirchhoff, W. H. Microwave Spectrum, Ground State Structure, and Dipole Moment of Thioformaldehyde. *J. Mol. Spectrosc.* **1971**, *39*, 136–145.
- (171) Fung, K. H.; Ramsay, D. A. Doppler-free Stark Spectra of the 401 Band of the SA1A2–X1A1 System of Thioformaldehyde. *Mol. Phys.* **1996**, *88*, 997–1004.
- (172) Freeman, D. E.; Klemperer, W. Dipole Moments of Excited Electronic States of Molecules: The  $^1A_2$  State of Formaldehyde. *J. Chem. Phys.* **1964**, *40*, 604–605.
- (173) Freeman, D. E.; Klemperer, W. Electric Dipole Moment of the  $^1A_2$  Electronic State of Formaldehyde. *J. Chem. Phys.* **1966**, *45*, 52–57.
- (174) Bridge, N. J.; Haner, D. A.; Dows, D. A. Electric-Field-Induced Spectra: Theory and Experimental Study of Formaldehyde. *J. Chem. Phys.* **1968**, *48*, 4196–4210.
- (175) Mentall, J. E.; Gentieu, E. P.; Krauss, M.; Neumann, D. Photoionization and Absorption Spectrum of Formaldehyde in the Vacuum Ultraviolet. *J. Chem. Phys.* **1971**, *55*, 5471–5479.
- (176) Suto, M.; Wang, X.; Lee, L. C. Fluorescence from VUV excitation of formaldehyde. *J. Chem. Phys.* **1986**, *85*, 4228–4233.
- (177) Matsuzawa, N. N.; Ishitani, A.; Dixon, D. A.; Uda, T. Time-Dependent Density Functional Theory Calculations of Photoabsorption Spectra in the Vacuum Ultraviolet Region. *J. Phys. Chem. A* **2001**, *105*, 4953–4962.
- (178) Jensen, P.; Bunker, P. R. The Geometry and the Out-Of-Plane Bending Potential Function of Thioformaldehyde in the  $\tilde{A}^1A_2$  and  $\tilde{a}^3A_2$  Electronic States. *J. Mol. Spectrosc.* **1982**, *95*, 92–100.
- (179) Dunlop, J. R.; Karolczak, J.; Clouthier, D. J.; Ross, S. C. Pyrolysis Jet Spectroscopy: The  $S_1 - S_0$  Band System of Thioformaldehyde and the Excited-State Bending Potential. *J. Phys. Chem.* **1991**, *95*, 3045–3062.
- (180) Dixon, R. N.; Webster, C. R. The Determination of the Electric Dipole Moment of  $H_2CS$  in the A1A2 Excited State Using Dye-Laser Electric Field Spectroscopy. *J. Mol. Spectrosc.* **1978**, *70*, 314–322.
- (181) Dixon, R. N.; Gunson, M. R. The Dipole Moment of Thioformaldehyde in its Singlet and Triplet  $\pi^* - n$  Excited States. *J. Mol. Spectrosc.* **1983**, *101*, 369–378.
- (182) Judge, R. H.; Drury-Lessard, C. R.; Moule, D. C. The Far Ultraviolet Spectrum of Thioformaldehyde. *Chem. Phys. Lett.* **1978**, *53*, 82–83.
- (183) Saito, S.; Takagi, K. Microwave Spectrum of Nitroxy. *J. Mol. Spectrosc.* **1973**, *47*, 99–106.
- (184) Dixon, R. N.; Noble, M. The Dipole Moment of HNO in its A1A $^{\prime}$  Excited State Determined using Optical-Optical Double Resonance Stark Spectroscopy. *Chem. Phys.* **1980**, *50*, 331–339.
- (185) Takagi, K.; Suzuki, T.; Saito, S.; Hirota, E. Microwave Optical Double Resonance of HNO: Dipole Moment of HNO in A1A $^{\prime}$ (100). *J. Chem. Phys.* **1985**, *83*, 535–538.
- (186) Johns, J. W. C.; McKellar, A. R. W. Laser Stark Spectroscopy of the Fundamental Bands of HNO ( $\nu_2$  and  $\nu_3$ ) and DNO ( $\nu_1$  and  $\nu_2$ ). *J. Chem. Phys.* **1977**, *66*, 1217–1224.
- (187) Scuseria, G. E.; Duran, M.; MacLagan, R. G. A. R.; Schaefer, H. F. Halocarbenes CHF, CHCl, and CHBr: Geometries, Singlet-Triplet Separations, and Vibrational Frequencies. *J. Am. Chem. Soc.* **1986**, *108*, 3248–3253.
- (188) Wagner, M.; Gamperling, M.; Braun, D.; Prohaska, M.; Hüttner, W. Rotational Transitions and Electric Dipole Moment of Fluorocarbene, HCF. *J. Mol. Struct.* **2000**, *517–518*, 327–334.
- (189) Kakimoto, M.; Saito, S.; Hirota, E. Doppler-Limited Dye Laser Excitation Spectroscopy of HCF. *J. Mol. Spectrosc.* **1981**, *88*, 300–310.
- (190) Lu, T.; Hao, Q.; Wilke, J. J.; Yamaguchi, Y.; Fang, D.-C.; Schaefer, H. F. Silylidene ( $SiCH_2$ ) and its Isomers: Anharmonic Rovibrational Analyses for Silylidene, Silaacetylene, and Silavinylidene. *J. Mol. Struct.* **2012**, *1009*, 103–110.
- (191) Smith, T. C.; Evans, C. J.; Clouthier, D. J. Discovery of the Optically Forbidden  $S_1 - S_0$  Transition of Silylidene ( $H_2C=Si$ ). *J. Chem. Phys.* **2003**, *118*, 1642–1648.
- (192) Harper, W. W.; Waddell, K. W.; Clouthier, D. J. Jet Spectroscopy, Structure, Anomalous Fluorescence, and Molecular Quantum Beats of Silylidene ( $H_2C=Si$ ), the Simplest Unsaturated Silylene. *J. Chem. Phys.* **1997**, *107*, 8829–8839.
- (193) Hilliard, R. K.; Grev, R. S. The Excited Electronic States of  $H_2CSi$ . *J. Chem. Phys.* **1997**, *107*, 8823–8828.